

Air Force Institute of Technology

AFIT Scholar

Theses and Dissertations

Student Graduate Works

3-1995

Analysis of Heads-Up Display Quickening Versus Handling Qualities

Gary M. Konnert

Follow this and additional works at: <https://scholar.afit.edu/etd>



Part of the [Aviation Commons](#), and the [Graphics and Human Computer Interfaces Commons](#)

Recommended Citation

Konnert, Gary M., "Analysis of Heads-Up Display Quickening Versus Handling Qualities" (1995). *Theses and Dissertations*. 6346.

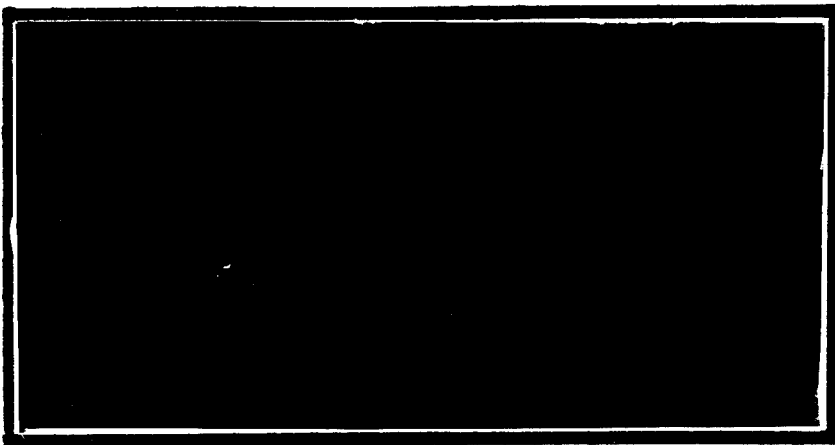
<https://scholar.afit.edu/etd/6346>

This Thesis is brought to you for free and open access by the Student Graduate Works at AFIT Scholar. It has been accepted for inclusion in Theses and Dissertations by an authorized administrator of AFIT Scholar. For more information, please contact AFIT.ENWL.Repository@us.af.mil.

DTIC
ELECTE
MAY 5 1995
S **C** **D**



DECLASSIFICATION STATEMENT X
Approved for public release
Distribution Unlimited



DEPARTMENT OF THE AIR FORCE
AIR UNIVERSITY
AIR FORCE INSTITUTE OF TECHNOLOGY

Wright-Patterson Air Force Base, Ohio

DTIC QUALITY INSPECTED 1

AFIT/GAE/ENY/95M-01

Accession For	
NTIS CRA&I	<input checked="" type="checkbox"/>
DTIC TAB	<input type="checkbox"/>
Unannounced	<input type="checkbox"/>
Justification	
By _____	
Distribution /	
Availability Codes	
Dist	Avail and/or Special
A-1	

**Analysis of Heads-Up Display Quickening
Versus Handling Qualities**

THESIS

Gary M. Konnert, Captain, USAF

AFIT/GAE/ENY/95M-1

Approved for Public Release; Distribution Unlimited.

19950503 095

Disclaimer Statement

The views expressed in this thesis are those of the author and do not reflect the official policy or position of the Department of Defense or the U. S. Government.

AFIT/GAE/ENY/95M-01

ANALYSIS OF HEADS-UP DISPLAY QUICKENING
VERSUS HANDLING QUALITIES

THESIS

Presented to the Faculty of the School of Engineering
of the Air Force Institute of Technology
Air Force Education and Training Command
In Partial Fulfillment of the
Requirements for the Degree of
Master of Science in Aeronautical Engineering

Gary M. Konnert, B.S.

Captain, USAF

March 1995

Approved for Public Release; Distribution Unlimited.

Preface

The purpose of this study was to develop an analytical method of obtaining an optimal quickening time constant for a flight path marker. Up to this point, the time constants were determined by simulator studies requiring a great deal of time and resources. By producing an analytical method for choosing the time constant, quickening can become more affordable and enhance the use of modern Heads-Up Displays.

A relatively simple solution to this problem was developed. Analytically, the results were good. The most promising and realistic results came from the flight test. Flight testing revealed some surprising results, but did verify that the solution developed was a beneficial, less expensive method.

In performing this analysis and flight testing I had a great deal of help from others. I am indebted to my faculty advisor, Dr. Brad Liebst, for his guidance and patience. Dr John Reising and Sqdn Ldr Bob Munns of Wright Labs offered the original idea for the study and continuous support. I also want to thank Lt Col Dan Gleason for his help setting up the flight test. Flight testing itself could not have been done without the help of CALSPAN's Lou Knotts and my fellow classmates at the USAF Test Pilot School, Capt Ken Plaks and Capt Jeff Wallace. Most of all I want to thank my wife, Laura, and kids, Kathy and Thomas, for putting up with those late nights and long hours.

Gary M. Konnert

Table of Contents

	Page
Preface	ii
List of Figures	vi
List of Tables	viii
List of Abbreviations	ix
Abstract	x
I. Introduction	1-1
Motivation	1-1
Objectives	1-4
Method	1-4
Limitations	1-6
II. Background	2-1
Quickening	2-1
History	2-6
III. Handling Qualities	3-1
Handling Qualities Ratings	3-1
Modifying Handling Qualities	3-4
Handling Qualities Prediction	3-4
Neal-Smith Method	3-4
Root Mean Square Method	3-7
Optimal Control Model	3-12
IV. Experimental System	4-1
Display	4-1
Pilot	4-3
Optimal Control Model	4-3

	Page
Aircraft	4-3
Flight Path Angle to Pitch Attitude	4-4
V. Quickening Time Constant Analysis	5-1
VI. F-16 Model Case Study	6-1
Case One	6-3
Case Two	6-5
Overall Results	6-8
VII. Flight Test	7-1
Test Item Description	7-1
Test Objectives	7-4
Test Procedures	7-4
ILS Offset Approach	7-5
Low Altitude Flight Path Tracking	7-6
Aim-Off Point Tracking	7-7
Data Processing, Reduction, and Analysis	7-8
Test Results	7-9
Flight Test Conclusions and Recommendations	7-17
VIII. Findings and Conclusions	8-1
Appendix A: Optimal Control Model Parameters	A-1
Appendix B: F-16 Case Models	B-1
Appendix C: Low Order Equivalent Systems Matching Matlab® M-Files	C-1
Appendix D: Pilot Transfer Functions	D-1
Appendix E: Case Study Root Mean Square Results	E-1
Appendix F: Cooper-Harper Rating Criteria	F-1
Appendix G: LAHOS Aircraft Configurations and Pilot Transfer Functions for Root Mean Square Database	G-1
Appendix H: Root Mean Square (RMS) Flight Test Handling Quality Regions	H-1

	Page
Bibliography	BIB-1
Vita	VIT-1

List of Figures

Figure	Page
1.1. Baseline Configuration	1-5
1.2. Quickened System	1-5
2.1. Washout Filter Example Bode Plots	2-6
2.2. Washout Filter Example Step Time Response	2-7
3.1. Cooper-Harper Rating Scale	3-3
3.2. Neal-Smith Closed Loop System	3-5
3.3. LAHOS RMS System	3-7
3.4. LAHOS Database RMS versus Cooper-Harper Ratings (CHR)	3-11
3.5. Block Diagram Optimal Control Model	3-12
4.1. Flight Path Tracking System	4-1
5.1. System Open Loop Aircraft	5-1
6.1. Case One Root Mean Square (RMS) Results	6-4
6.2. Case Two Root Mean Square(RMS) Results	6-7
6.3. Quickening Time Constant Scheduling Curves	6-10
6.4. Theoretical Optimum Quickening Time Constant Bias	6-10
7.1. Heads-Up Display Tracking Task Command	7-7
7.2. HUD Tracking Root Mean Square (RMS) Summary	7-14
7.3. Aim Point Tracking Root Mean Square (RMS) Summary	7-14
7.4. ILS Tracking Root Mean Square (RMS) Summary	7-15
B.1. F-16 Longitudinal Flight Control System	B-2

Figure	Page
H.1. HUD Tracking Flight Test RMS Handling Quality Regions	H-2
H.2. Aim Point Tracking Flight Test RMS Handling Quality Regions	H-2
H.3. ILS Tracking Flight Test RMS Handling Quality Regions	H-3

List of Tables

Table	Page
3.1. Neal-Smith System Criteria -3dB Closed-Loop Droop	3-6
6.1. Case Study Quickening Time Constants	6-2
6.2. Case Study Density Ratio versus Pressure Ratio for Quickening Time Constants	6-2
6.3. Case One Optimal Control Model Cooper-Harper Predictions	6-3
6.4. Neal-Smith Pilot Rating Predictions	6-6
7.1. Quickening Time Constants	7-2
7.2. Rank Ordered Time Constant Summary Best (Top) to Worst (Bottom)	7-11
7.3. Cooper-Harper Ratings Summary	7-12
7.4. Root Mean Square Analysis Group Summary	7-13
7.5. Rank Ordered Overall Paired Comparison Results	7-15
E.1. Case One Root Mean Square (RMS) Results Mach number = 0.24 Pressure Altitude = 1,000 feet	E-2
E.2. Case Two Root Mean Square (RMS) Results Mach number = 0.60 Pressure Altitude = 1,000 feet	E-2
G.1. LAHOS CHR 1-3 Aircraft Configurations Used for Database	G-2
G.2. Neal-Smith Pilot Models for LAHOS CHR 1-3	G-3
G.3. LAHOS CHR 4-6 Aircraft Configurations Used for Database	G-4
G.4. Neal-Smith Pilot Models for LAHOS CHR 4-6	G-5
G.5. LAHOS CHR 7-10 Aircraft Configurations Used for Database	G-6
G.6. Neal-Smith Pilot Models for LAHOS CHR 7-10	G-6

List of Abbreviations

AFB	Air Force Base
AFFTC	Air Force Flight Test Center
AFIT	Air Force Institute of Technology
AGL	Above Ground Level (feet)
CA	California
CDAMQ	Climb/Dive Angle Marker Quickening
CDLQ	Climb/Dive Ladder Quickening
CDM	Climb Dive Marker
CHR	Cooper-Harper Rating
DAS	Data Acquisition System
dB	Decibel ($20 \cdot \log_{10} x$)
FCS	Flight Control System
FPM	Flight Path Marker
FPMQ	Flight Path Marker Quickening
HUD	Heads-Up Display
IFR	Instrument Flight Rules
ILS	Instrument Landing System
IMC	Instrument Meteorological Conditions
KBF	Kalman Bucy Filter
KIAS	Knots Indicated Air Speed (nm / hr)
LQR	Linear Quadratic Regulator
NASA	National Aeronautics and Space Administration
OCM	Optimal Control Model
PA	Power Approach
PA	Pressure Altitude (feet)
RMS	Root Mean Square
RPM	Revolutions Per Minute (%)
SAS	Stability Augmentation System
SISO	Single Input Single Output
STI	Systems Technology, Inc.
TLR	Technical Letter Report
TPS	USAF Test Pilot School
USAF	United States Air Force
VISTA	Variable In-flight Simulator Test Aircraft
VSS	Variable Stability System

Abstract

This study investigated an analytical means of selecting the quickening time constant for the standardized Heads-Up Display flight path marker. Good results were obtained. The theoretically determined time constant allowed a faster, less resource intensive means of selecting the quickening time constant.

A closed-loop pilot-aircraft flight path command following system with quickening in the forward loop was created to develop a theoretically determined time constant. The theoretically best time constant for pilot-aircraft handling qualities was equal to the airframe pitch attitude high frequency zero time constant, T_{θ_2} . Theory was validated using two F-16 case study models and flight test. Comparison of the quickening effects on handling qualities were done by using Neal-Smith, Optimal Control Modeling, Root Mean Square method, and Cooper-Harper Ratings.

The theoretically determined time constant generated desirable handling qualities. Flight test indicated an empirical, more labor intensive method yielded better handling qualities, even though paper analysis indicated the theoretical method was better. Further study is required to determine why the empirical method generated better results during flight test. The theoretically determined time constant gave slightly lower handling qualities, but was less costly to implement than the empirical method. For this reason T_{θ_2} should be used for quickening.

ANALYSIS OF HEADS-UP DISPLAY QUICKENING VERSUS HANDLING QUALITIES

1. Introduction

Motivation. Heads-Up Displays (HUDs) present flight information to pilots without having to look inside the cockpit. Generally, this is done by projecting the information onto a glare shield mounted combining glass. The information appears projected onto the canopy or windshield focused at infinity. This enables the pilot to see the information while viewing the outside world. Spending less of his attention inside the cockpit allows the pilot to concentrate on what is happening outside the aircraft. This factor enhances nearly every phase of flight or task given the pilot, clearing (looking for other aircraft), delivering weapons, or landing the aircraft.

Originally, the HUD was designed for weapons delivery. Consequently, each contractor for an aircraft developed their own symbology for use with the HUD. This factor leads to a wide diversity of HUDs each with its own peculiarities. Developed without the human factors that went into presentation of cockpit primary flight reference data, some HUDs are more effective in certain arenas than others. Information other than weapons delivery data displayed on the HUD generally includes flight references used for aircraft control. Pilots increasingly rely on this information since it allows them to keep their attention outside the aircraft.

Late in 1986 two F-16 mishaps highlighted the HUD's lack of design as a primary flight reference. Yet, the advantages of using the HUD as a primary flight reference are overwhelming. The FAA's certification of aircraft for manual Category III ILS use based on a HUD is one documented example. (6:236) (Category III certification means that the aircraft can land in weather as bad as zero ceiling and 700 foot Runway Visual Range. Until 1987 this category required totally automated systems that were very difficult to design.)

In response to the mishaps the USAF began studying the symbology required for an Instrument Flight Rules (IFR) standardized HUD design. Current HUDs in the Air Force remain uncertified for such use. Further accidents implicating pilot performance degradations due to poor displays/symbologies in Instrument Meteorological Conditions (IMC) intensified research. In 1990 a standardized HUD for use as a primary reference during IMC was developed. Testing of this standardized HUD began in 1991. The aim is to develop a military standard for the design of Heads-Up Displays. The culmination of this research is MIL-STD-1787B.

Future aircraft will follow MIL-STD-1787B guidance. Current aircraft could conceivably be retrofitted. Yet, there is one important symbol presently implemented only after much empirically derived testing, the flight path marker. The flight path marker (FPM) designates the current path or velocity vector followed by an aircraft. On a HUD the symbol is read in relation to the outside environment. The FPM's usefulness as a primary control reference is one reason for the HUD's widespread utilization. Traditional pitch reference displays require the pilot to integrate pitch attitude, vertical velocity, and angle-of-attack to determine flight path. Having the

flight path displayed directly reduces the pilot's mental workload. This reduction directly affects an aircraft's handling qualities. In addition a direct variant of the FPM is the Climb/Dive Marker (CDM) which shows the vertical flight path relative to a graduated ladder. The Climb/Dive Marker differs from the FPM in that the symbol is restricted to the vertical axis. The CDM is important in unusual attitude recoveries. (11:Sec A, 8)

Both Flight Path Marker and Climb/Dive Marker usage requires quickening. Quickening compensates for the effects of an aircraft's inertia. (11:Sec A, 8) Without this compensation the response of the symbols would require interpretation or anticipation by the pilot. Quickening makes the Flight Path Marker or Climb/Dive Marker more predictable. An unquickened CDM or FPM will lag the actual final position of the aircraft's position because of inertia. If the pilot commands a 5° climb, the FPM or CDM lags the aircraft pitch and initially overshoots when 5° is reached. This response demands the pilot integrate the lag into his performance. While this integration can be done and done well with experience, it increases the pilot's workload. Theoretically, these dynamics could even cause the pilot to destabilize the aircraft (ie. provoke a Pilot Induced Oscillation). Quickening makes the FPM more predictable by adding the lead compensation for the pilot.

Quickening is an important aspect of the standardized Heads-Up Display. Through its impact on the HUD, quickening influences handling qualities of an aircraft. The form of the standard HUD quickening is set by Mil-Std-1787B, but not the amount. The time constant or amount for the best quickening on each aircraft is

unknown except through empirical testing. This requirement translates into increased time and money required for implementing quickening. No analytical means exists up to now for determining the standardized HUD quickening time constant.

Objectives. The general objective of this project is to develop a useful means of determining the quickening time constant required for the Flight Path Marker of the standardized Heads-Up Display. This overall goal is accomplished by meeting the following specific objectives:

1. Develop analytical means to choose time constants for the given quickening algorithm.
2. Investigate effects of the quickening algorithm on handling qualities.
3. Compare Neal-Smith classical handling qualities criteria with quickened aircraft handling qualities.
4. Implement analytical quickening optimization for F-16.
5. Validate analytic method by comparing results with previously constructed quickening and simulations.
6. Validate analytical quickening optimization and effect on handling qualities through flight-test.
7. Conduct flight-testing and publish data from test to aid further research in the area.

All these objectives were accomplished.

Method. To achieve the goals of this project the following methodology is pursued:

1. A baseline system is built of a plant and pilot without quickening. This arrangement consists of a Neal-Smith type configuration for flight path. See Figure 1.1. The pilot minimizes the error between the commanded flight path angle and the

actual flight path angle feeding through the HUD. The pilot is modeled using the Systems Technology, Inc. (STI) Optimum Control Model (OCM) or a Neal-Smith pilot model.

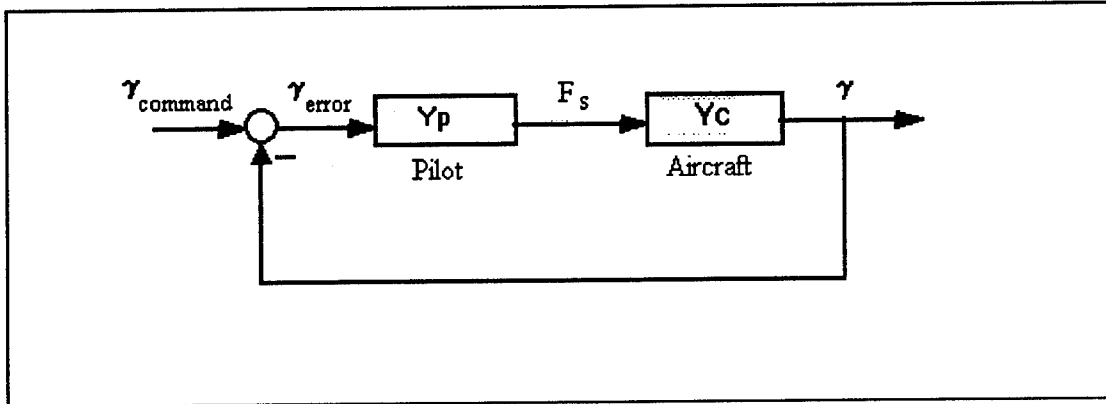


Figure 1.1 Baseline Configuration

2. Measurements are taken from the baseline system and used for comparison with the quickened system. These include Root Mean Square (RMS) values of control rate and flight path error as performance and workload measures.

3. The quickened system is constructed by placing the standard HUD quickening algorithm in the forward path. See Figure 1.2. In this configuration the pilot minimizes the error (γ_{error}) between the commanded flight path angle ($\gamma_{command}$) and the compensated flight path angle displayed ($\gamma_{display}$) on his HUD.

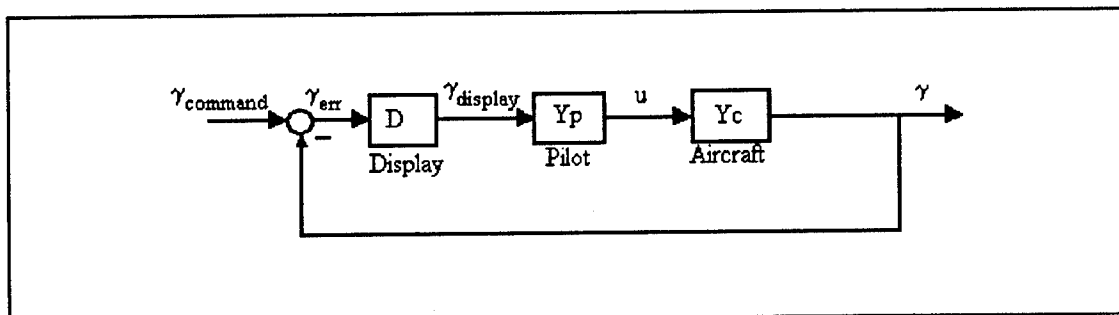


Figure 1.2 Quickened System

4. Analyze the quickened system to yield a theoretically optimum quickening time constant.

5. After finding the optimum time constant, measurements are taken to include RMS values. These criteria are compared against various time constants and the baseline system to evaluate quickened handling qualities performance.

6. Repeat the analysis for an actual aircraft model, the F-16. This is done to show that the method for optimization works for a realistic configuration.

7. Validate the F-16 case results with the empirically determined quickening time constant.

8. Flight testing extends the validation to the real world. Flight test configurations include the theoretically optimum and empirically determined quickening time constants. Compare results between the two values and a cross-section of other time constants.

Limitations. There are several limitations inherent in this study. First, the study is restricted to the vertical axis. Not only does this restriction reduce complexity of the task, it also simplifies handling qualities evaluations. Few methods exist for studying multi-axis handling quality ratings. Most of the existing database involves single axis ratings only, among which the vertical axis predominates.

Secondly, all components are linearized. The equations of motion employed for the aircraft and its control system are quasi-steady state linearizations. As the aircraft departs from this linearized flight condition, the equations are less accurate. Use of aircraft low order equivalent systems also induces minor errors.

Pilot modeling using OCM and Neal-Smith methods also assumes approximation of a highly non-linear human operator. While human beings are definitely not linear, studies have shown that their behavior can be successfully approximated by these methods. The primary feedback parameters used by the pilot are the flight path angle and the flight path angle rate. More cues are available to the pilot, but for tasks demanding flight path control these two values are considered primary.

Next, the effects of control stick sensitivity and the delays inherent in the HUD are assumed to be constant between the baseline system and the quickened one. Both control stick sensitivity and the delay in the HUD's displaying CDM and FPM symbols affect handling qualities. However, since these factors are constant between the two systems, comparisons of handling qualities should be unaffected.

Last but not least, the given quickening algorithm directed by the standardized HUD is only a first order approximation for a higher order system. Therefore, the algorithm does not perfectly compensate the FPM movement. The format selected is only used for fighter type aircraft without large center of gravity changes and at pitch attitudes less than 30 degrees.

II. BACKGROUND

Quickening. Quickening consists of a simple lead compensator that aids the usefulness of an operator display. In this instance the algorithm or transfer function calculates an estimate of instantaneous Climb/Dive Marker or Flight Path Marker displacement caused by the aircraft dynamics. (11:Sec A, 8) These dynamics consist of lag due to aircraft inertia. The primary goal is to stabilize the symbology to make it more predictable and easier to use. Hence, lead compensation is used to offset inherent lags. The transfer function for the quickening defined in Mil-Std-1787B, *Aircraft Display Symbology*, is composed of two different forms. Of these two slightly different forms only one will be examined by this thesis.

The reasoning for two different forms follows from the two different markers, CDM and FPM, being quickened. A Climb/Dive Marker displays the current climb/dive angle, similar to a vertical axis flight path marker. The Climb/Dive Marker symbol is read against the Climb/Dive Ladder. As such the CDM is aircraft referenced. These dynamics lead to Euler or body axis pitch angle rates being used for quickening. This necessity can be observed by thinking of a high-g turn. If only body axis pitch angles were used which change very little, not much compensation would be provided. A compensator using body axis pitch rates would allow compensation throughout maneuvering flight. (11:Sec A, 9) This methodology was born out in flight testing at the Naval Flight Test Center. For approach and landing an

exception was noted, however. Flight testing showed that using angles instead of rates was preferable. (7:8-6)

The Flight Path Marker is read against the outside horizon. As such the symbol is earth referenced. For this reason compensation should be done with pitch attitude. Again, this fact was born out by flight testing. The restriction on this type lies in small angles. When large angles are encountered then reverting to a pitch rate compensator is preferable. In summary, the FPM should use pitch angle compensation for low pitch angles and pitch rate compensation for high pitch angles.

Comparatively, the CDM should use pitch rate compensation for normal flight with the exception of approach and landing. During this phase of flight the pitch angle filter should be used.

Mil-Std-1787B sets the format for the quickening of the standardized Heads Up Display (HUD). The two compensators used for the FPM and CDM are a pitch angle and pitch rate lead compensator scheduled and blended based on aircraft pitch angle. The exact form of the pitch angle filter is Equation (1).

$$\Delta\gamma = Q1 = G \cos\phi \frac{s}{s + \frac{1}{\tau}} \theta \quad (1)$$

The exact form of the pitch rate filter is Equation (2).

$$\Delta\gamma = Q2 = G_1 \frac{1}{s + \frac{1}{\tau}} q \quad (2)$$

where

$\Delta\gamma$ = flight path angle quickening addition
 G, G_1 = quickener gains
 ϕ = aircraft roll angle (degrees)
 θ = aircraft pitch angle (degrees)
 τ = time constant (seconds)
 q = aircraft body axis pitch rate (degrees / second)
 s = Laplace complex frequency variable

Blending the two filters is required when used in actual aircraft to avoid too sharp a changeover between the modes. A good control system or compensator should be transparent to the pilot. According to Mil-Std-1787B this task is accomplished in the following manner. During normal flight:

$$\begin{aligned} \text{FPMQ} = \text{CDLQ} &= Q1 \times B1 + Q2 \times B2 & (3) \\ \text{CDAMQ} &= Q2 \end{aligned}$$

For ILS mode or landing gear down:

$$\text{FPMQ} = \text{CDAMQ} = \text{CDLQ} = Q1 \times B1 + Q2 \times B2 \quad (4)$$

where

$$B2 = \begin{cases} 0 & |\theta| \leq 30^\circ \\ \frac{|\theta| - 30^\circ}{55^\circ - 30^\circ} & 30^\circ < |\theta| < 55^\circ \\ 1 & |\theta| \geq 55^\circ \end{cases} \quad (5)$$

and

$$B1 = \begin{cases} 1 & |\theta| \leq 30^\circ \\ 1 - B2 & 30^\circ < |\theta| < 55^\circ \\ 0 & |\theta| \geq 55^\circ \end{cases} \quad (6)$$

where

FPMQ = Flight Path Marker Quickening
CDLQ = Climb/Dive Ladder Quickening
CDAMQ = Climb/Dive Angle Marker Quickening
Q1 = Pitch Angle Filter
Q2 = Pitch Rate Filter
 θ = Aircraft Pitch Angle (degrees)

Once the quickening component, FPMQ or CDAMQ, is computed then this component is added to the raw flight path angle. This summation is the symbol then presented on the HUD. Therefore the actual FPM display consists of Equation (7).

$$\text{FPM} = \gamma + \text{FPMQ} \quad (7)$$

where

FPM = Flight Path Marker (degrees)
 γ = Flight Path Angle (degrees)
FPMQ = Flight Path Marker Quickening (degrees)

The scope of this thesis concerns itself with only the pitch angle filter for several reasons. Primarily, the pitch angle filter is seen as the most important of the quickening types. The FPM's usefulness manifests itself in tasks such as approach and landing, air-to-ground weapons delivery, and terrain avoidance/terrain following. During up and away flight or air-to-air weapons employment the FPM is not as critical and is probably replaced on the HUD by specialized weapons or navigation symbology. This low altitude use of the FPM narrows the pitch region to generally small angles. Additionally the CDM uses the pitch angle filter during approach and landing, another low pitch angle area. The majority of important tasks involve small angles and the use of pitch attitude quickening.

Casting the form of the filter leaves only two variables open for exploration. These two are the gain and the time constant. Currently, the largest area unexplored concerns the time constant. Flight testing empirically derived an optimum gain of 0.7 with this type filter. (5:27) Time constants, on the other hand, while determined empirically in flight test for a particular aircraft cannot be generalized as easily to other aircraft. This factor leads to the present necessity of using high fidelity simulators and actual test flights to determine time constants for each aircraft employing the standard HUD. This necessity could be difficult if the aircraft is still in the design process, not to mention expensive for updating current aircraft.

Mil-Std-1787B defines the quickening time constant by Equation (8). (7:Sec A, 10)

$$\tau = A + \frac{B}{V_t \sigma} \quad (8)$$

where

τ = Quickening Time Constant (seconds)

A, B = Constants

V_t = Aircraft's True Airspeed (feet per second)

σ = Relative Density Ratio

The two constants are the unknowns. By finding the time constant for two or more widely spaced values of true airspeed and relative density ratio (ie. wide values of dynamic pressure) in the flight envelope, A and B can be solved for simultaneously. This should give a reasonable fit for the aircraft throughout its envelope and allow the time constant to be scheduled. (5:27) Methods described in Chapter V discuss the selection of the time constant for a given aircraft and flight condition. From there,

determination of A and B constants allow a schedule for the aircraft to be developed or use of a look up table.

History. Quickening is not a widely known name, but the concept itself has been around for quite a while. Basically the quickening filter is a lead compensator more commonly recognized as a 'washout filter'. A washout filter operates by passing only transient inputs and zeroing out steady state and low-frequency inputs. Thus the filter effectively speeds up the transient response towards its steady state value. In addition 90° of phase lead is added at low frequencies. (3:529) These qualities are illustrated in Figure 2.1 and Figure 2.2 by the responses to an example washout filter with a time constant of 3 seconds. See Equation (9).

$$H(s) = \frac{s}{s + \frac{1}{3}} \quad (9)$$

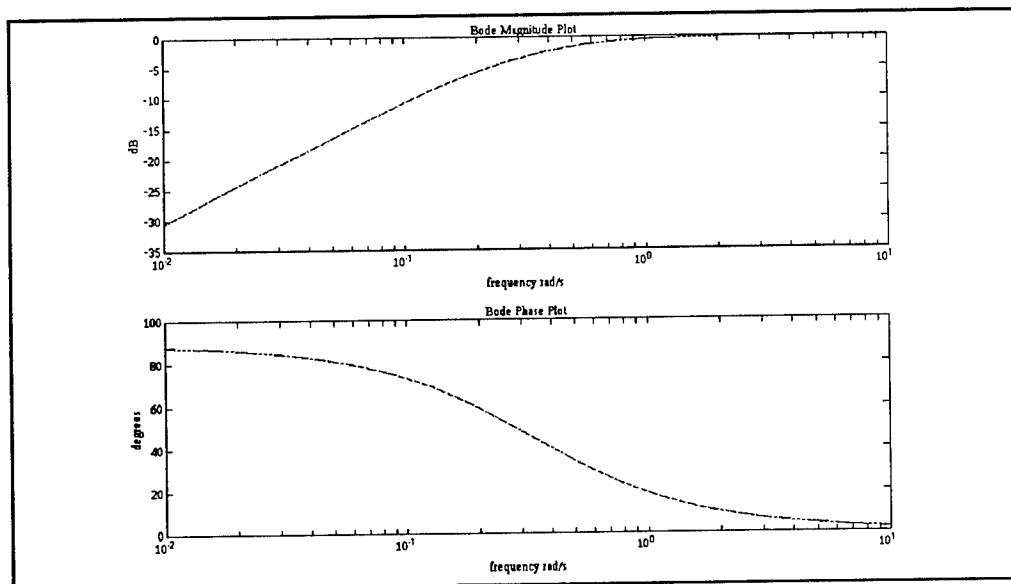


Figure 2.1 Washout Filter Example Bode Plots

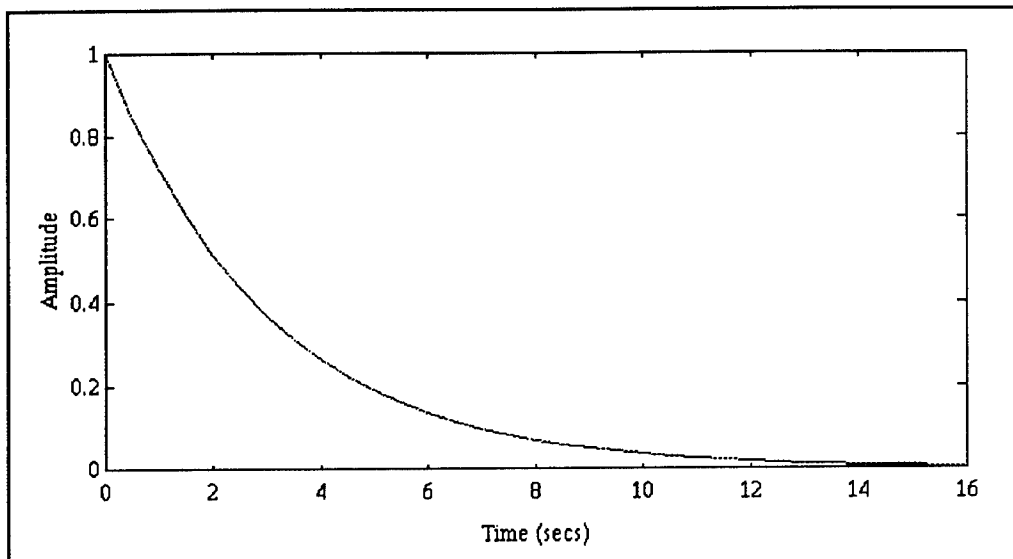


Figure 2.2 Washout Filter Example Step Time Response

By adding quickening or lead compensation of this form to the FPM and CDM the transient responses are speeded up. The settling time of the markers is decreased so that the time lag to reach the steady-state response is eliminated. From this characteristic comes the name "quickening." (7:8-6)

Several studies conducted document the fact that quickened displays enhance tracking tasks. (1,12) Primarily, this benefit comes from the additional lead supplied by the compensator which reduces operator workload and allows improved tracking. Other types of HUD quickening which were explored up to and including optimal control synthesis of active displays are included in references 1 and 12. The washout filter being studied by this project has been the subject of both British, Navy, and Air Force projects.

Originally studied by the British in 1989, a precursor to the standardized HUD format was tested on a T4 Harrier. The format included the HUD quickening algorithm presently recommended. The quickening and format specifics at the time were tuned to the Harrier. (5:1) Basing their work on this study, further investigations were made by the Navy and the Air Force. Test results at the Naval Air Test Center showed pilot workload and glidepath performance were significantly improved by the use of a quickened HUD and flight director display. These tests were only performed for the approach and landing task. The following recommendations resulted from these tests. For aircraft with weak control law augmentation such as a pitch Stability Augmentation System (SAS) and a washout lead filter, the quickening time constant should equal the angle of attack's settling time. Advanced control law aircraft were given no specific recommendations for time constants. The time constant can be fixed for the approach and landing task , but for other tasks should be scheduled with airspeed and altitude. (7)

Without FPM quickening, the FPM consistently required approximately one second to damp out. This bobbling required the pilot to add his own compensation. Quickening allows the pilot to neutralize his input when the FPM reaches the desired setting instead of leading the symbol. The Grumman F-14 Tomcat currently uses washout filter quickening in all flight regimes. This washout filter is the same type and implemented in the same manner as the one being investigated in this paper. The time constant is scheduled with airspeed. Typical values for the time constant range from 0.8 to 1.4. Currently certain Navy aircraft are already using quickened HUDs as Instrument Flight Rule (IFR) certified primary references. (7:Sec 8, 7-9)

The Air Force and NASA also built on this research. One such study, reference 4, highlights the interest in the area of HUD augmentation of the civilian sector. This study's experimental results showed limited improvement in tracking performance. These findings disagree with the norm. The majority of studies showed marked improvement with display augmentation such as quickening. All the studies agreed that too much augmentation will actually decrease performance. (4:6)

After researching these and other studies, the USAF's Armstrong and Wright Laboratories commissioned a team in 1990 to investigate HUD displays, to include quickening. The team selected several candidate formats and proceeded with testing. Selected HUD symbology was incorporated into a single suite. In 1991 the USAF established basic standards for instrument displays including a standardized HUD suite. After validation testing, the IFR capable HUD format found in Mil-Std-1787B was adopted for use as the standardized HUD. This is the HUD format being investigated.

III. Handling Qualities

Handling qualities are those characteristics of the pilot-aircraft configuration that determine the level of performance and required workload for a given task. These qualities are what should be optimized to obtain the design that will give the desired performance for the lowest pilot workload. The reader should keep this concept in mind as the quickening filter is examined.

The purpose of the filter being investigated is to enhance the pilot-aircraft system handling qualities. These handling qualities are categorized in several ways. The general categories in reference 12, Mil-Std-1797A, *Flying Qualities of Piloted Aircraft*, will be used along with the Cooper-Harper Rating scale. Several numerical methods such as Neal-Smith and Root Mean Square allow analytical approximations of these ratings and will be discussed in the following chapter.

Handling Qualities Ratings. The three general categories are Satisfactory, Acceptable, and Controllable. Satisfactory, sometimes known as level one, means the qualities are clearly adequate for the mission and that desired performance is achievable with no more than minimal pilot compensation. Acceptable means the system is adequate, but that some increase in pilot workload or degraded task performance or both exist. Acceptable is also known as level two. The final category, Controllable or level three, denotes the system is controllable even with excessive pilot

workload and/or inadequate performance for the task being evaluated. Note that controllable in this instance does not necessarily mean safe. (12:2)

Handling qualities are task dependent. A pilot-aircraft combination may have excellent handling qualities for up and away flight, but terrible approach and landing qualities. For this reason a handling quality rating has to be associated with a task. These tasks are generally divided by flight phase into three categories. Nonterminal flight phases that require rapid maneuvering, precision tracking, or precise flight path control are known as category A. Tasks such as ground attack, air-to-air combat, and terrain following are examples of category A. Nonterminal flight phases that use gradual maneuvers and do not require precision tracking are category B. Examples include climbs, cruise, and descents. The final phase, terminal flight, is characterized by gradual maneuvers and requires accurate flight path control. Takeoffs, landings, approaches, and go-arounds are representative of this category. (12:80-81)

The measure of the discussed handling quality categories for all three flight phases in this paper is the Cooper-Harper Rating Scale. This scale, shown in Figure 3.1, provides subjective criteria for both pilot workload and task performance. Using these subjective criteria the rating scale uses a decision tree to lead a pilot or evaluator to a numerical rating. (12:12) The Cooper-Harper Rating Scale is prevalent in flight test use. These numerical values correspond to the handling quality categories explained. Satisfactory encompasses Cooper-Harper Ratings (CHR) of 1-3. Acceptable corresponds to CHRs of 4-6 and Controllable to CHRs of 7-9. The Cooper-Harper Scale also contains an additional category of CHR 10 or uncontrollable.

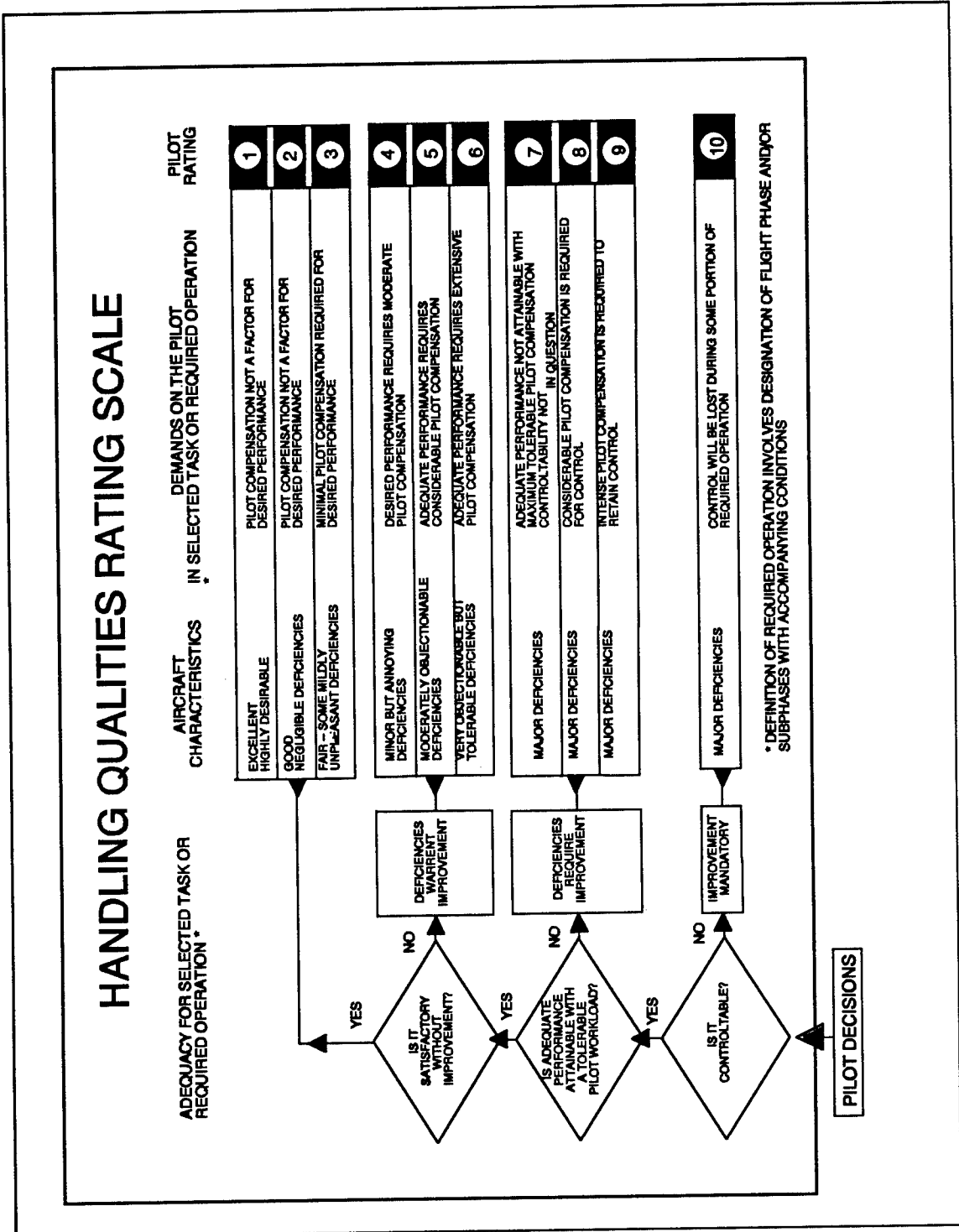


Figure 3.1 Cooper-Harper Rating Scale

Modifying Handling Qualities. Several means are available to influence pilot-aircraft handling qualities. The pilot is not subject to change by the designers or engineers. Therefore, the aircraft itself must be altered. Changing the physical form of the aircraft is generally quite expensive and must be done very early in the design process. Modifying the flight control system is a more palatable solution, but can still be very involved and costly. Finally, modifying the displays can achieve changes in handling qualities with a minimum of expense and relatively late in the aircraft's life cycle. This final alternative is the method by which quickening changes the pilot-aircraft handling qualities. To measure these design changes several analytic methods are available.

Handling Qualities Prediction. The three analytic methods used in this paper to predict handling quality categories and the associated Cooper-Harper Ratings are the Neal-Smith method, Root Mean Square (RMS) analysis, and the Optimal Control Model (OCM). These methods yield only approximations of the rating levels because of the nonlinearities inherent in the pilot and the aircraft. By using linear methods to analyze the pilot-aircraft combination, the best outcome for this nonlinear system and rating scale is a good approximation. Use of these approximations allow the prediction of pilot-aircraft performance prior to flight and the analysis of changes to the system. Most importantly these methods show the trends for the system and any changes.

Neal-Smith Method. A well established method, the Neal-Smith or Closed-Loop Criterion, has been used successfully to predict pitch attitude control. This method uses a closed-loop system with negative unity feedback and the forward path

consisting of the pilot and aircraft-flight control system. See Figure 3.2. (12:237)

Designed for pitch attitude tracking, this method does not normally address flight path control. However, the criteria as designed should operate with other command following closed-loop servomechanisms. With the flight path marker display on the HUD the pilot now has direct flight path feedback just as for pitch. Instead of the pilot integrating pitch to get the flight path as happens without a flight path marker, he now compensates flight path directly just as a servomechanism does. This allows the use of Neal-Smith criteria.

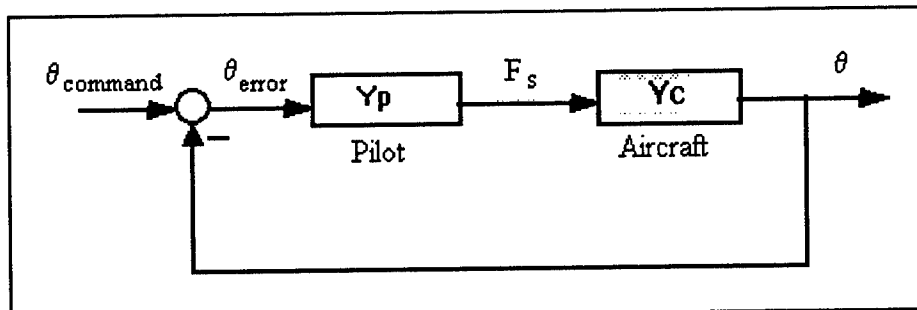


Figure 3.2 Neal-Smith Closed Loop System

The Neal-Smith criteria system has two basic components, the pilot and the aircraft-flight control system. The pilot transfer function used for this paper is the lower order pilot model. This transfer function assumes the form of Equation (10) where K_p , T_{p1} , and T_{p2} values are unlimited. Note that a .25 second pure time delay

$$Y_p = K_p e^{-.25s} \frac{(T_{p1}s+1)}{(T_{p2}s+1)} \quad (10)$$

is used to represent the pilot neuromuscular delays. For this paper the transfer function is a pilot force output to an error signal input. The second component, Y_c ,

is the aircraft dynamics. This transfer function is the combined pilot force input to aircraft response output. Importantly, this transfer function includes not only the aircraft's dynamics, but the flight control system as well.

Given this overall system in Figure 3.2, the handling qualities predictions are based on the ability to attain a specified bandwidth defined as a closed-loop phase of -90 degrees with no more than a -3 decibel closed-loop droop. Closed-loop resonance is restricted to a specified value. The values of the bandwidth and closed-loop resonance depend on the flight phase and handling quality level. See Table 3.1. Note that the definition for the controllable handling quality level is based on amplitude time to double and not closed-loop droop and resonance. These qualities for the system are over the frequency range of 0 to 10 radians per second. (12:237)

Table 3.1
Neal-Smith System Criteria
-3dB Closed-Loop Droop

FLIGHT PHASE	BANDWIDTH (rad/sec)	HANDLING QUALITY LEVEL	CLOSED-LOOP RESONANCE (dB)
Category A	3.5	Satisfactory	3
Category B	1.5	Acceptable	9
Landing	2.5	Controllable	≥ 6 seconds time to double
Other Category C	1.5		

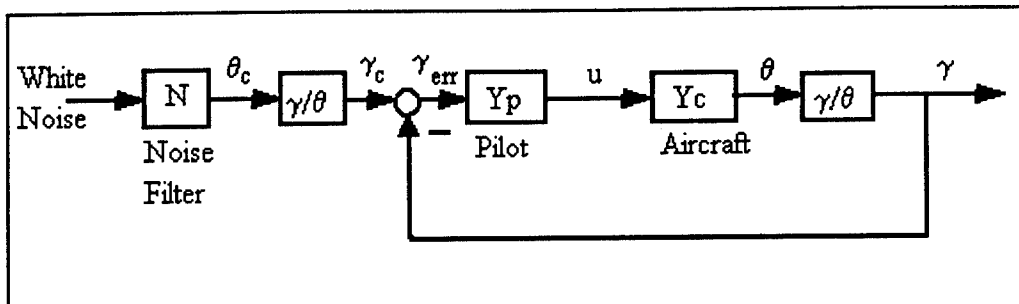


Figure 3.3 LAHOS RMS System

Root Mean Square Method. The second method for determining handling quality trends is the Root Mean Square (RMS) method. This method uses a combination of RMS measurements to quantify performance and workload. Performance is linked to error RMS. The lower the error RMS, the better the task is performed. Workload is measured by the pilot input rate RMS. The harder the pilot works the larger the pilot's input rates. Together these two quantities give the handling quality of the aircraft for a given task. By graphing the error RMS versus the pilot input rate RMS of the system for a task, handling qualities trends and levels can be identified. General trends can be identified without a database. With a database of actual pilot ratings and RMS measurements for the specific task, regions of different handling quality levels can be defined. The drawback to predicting the handling ratings is the requirement to have a database for the particular task being used. (1:9)

For analysis of the quickening effects, a database was constructed from *Display Systems Dynamics Requirements for Flying Qualities*, reference 1. The database is known as LAHOS. The LAHOS aircraft configurations were aircraft short period approximations combined with first order approximations of the control systems. An

approach and landing task was used to gather the actual pilot handling quality ratings of these configurations. See Figure 3.3 for the system description used to gather the RMS data.

The flight path angle to pitch attitude conversions were necessary due to the format of the database transfer functions and noise filter available. Equation (11) gives the noise filter used.

$$N = \frac{2}{s^2 + .5s + .25} \quad (11)$$

This filter approximates the frequency content of the IFR tracking task for a pitch variation of 4 degrees. Transformation to flight path angle was accomplished by use of Equation (12).

$$\frac{\gamma}{\theta} = \frac{\frac{1}{T_{\theta_2}}}{s + \frac{1}{T_{\theta_2}}} \quad (12)$$

where

θ - aircraft pitch angle (degrees)

γ - aircraft flight path angle (degrees)

T_{θ_2} - high frequency pitch attitude zero time constant (seconds)

This transformation holds as long as T_q (defined by Mil-Std-1797A) is not much less than T_{θ_2} , the high frequency pitch attitude zero time constant, as recommended by Mil-Std-1797A. (12:257-258) Pilot transfer functions are of two types. One is the Neal-Smith criteria pilot transfer function previously discussed and the other is an

optimal pilot model produced by STI. This latter pilot transfer function will be explained later in the chapter.

Error RMS for performance is the RMS value of the transfer function flight path angle error (γ_{error}) divided by commanded flight path angle ($\gamma_{command}$). Flight path angle error being defined as the difference between commanded flight path angle and the actual flight path angle. Displayed flight path is not used for the calculation since task performance is based on the aircraft response as opposed to the display's response. The pilot input rate RMS is simply the RMS value of the transfer function pilot input rate to commanded flight path angle. For calculating the RMS values commanded flight path angle consists of white noise passed through the noise filter and transformed to a flight path angle.

RMS values for the transfer functions are found by noting that for linear systems driven by white noise $w(t)$:

$$\begin{aligned} \dot{x} &= A*x+B*w(t) \\ y &= C*x \end{aligned} \quad (13)$$

where

$$\begin{aligned} E\{w(t)\} &= 0 \\ E\{w(t)*w^T(t+\tau)\} &= Q*\delta(\tau) \end{aligned} \quad (14)$$

$w(t)$ = Zero Mean Stationary White Gaussian Noise
 $P\{w(t)\}$ = Gaussian Probability Density
 Q = Constant Intensity Matrix for $w(t)$

The variance matrix \underline{X} defined as

$$\underline{X} = E\{[x(t) - E\{x(t)\}][x(t) - E\{x(t)\}]^T\} = E\{x(t) x(t)^T\} \quad (15)$$

$$\begin{aligned} P\{x(t)\} &= \text{Gaussian Probability Density} \\ E\{x(t)\} &= 0 \end{aligned}$$

is the solution of the following Lyapunov Equation

$$\mathbf{A} \underline{\mathbf{X}} + \underline{\mathbf{X}} \mathbf{A}^T + \mathbf{B} \mathbf{Q} \mathbf{B}^T = 0 \quad (16)$$

and the output variance matrix is

$$\underline{\mathbf{Y}} = \mathbf{E}\{[y(t) - E\{y(t)\}][y(t) - E\{y(t)\}]^T\} = \mathbf{E}\{y(t) y(t)^T\} = \mathbf{C} \underline{\mathbf{X}} \mathbf{C}^T \quad (17)$$

$$\begin{aligned} P\{y(t)\} &= \text{Gaussian Probability Density} \\ E\{y(t)\} &= 0 \end{aligned}$$

Because the filter is a SISO system, $\underline{\mathbf{Y}}$ is a scalar and is the output variance of the filter. The reader is directed to reference 10 for a discussion of RMS response of linear systems driven by white noise. The RMS value is then simply the square root of the variance.

$$RMS = \sigma = \sqrt{\underline{\mathbf{Y}}} \quad (18)$$

The results for this database showing RMS values and handling quality ratings are in Figure 3.4. Note that the controllable level region, CHR 7-9, was undefined because of the limited data available. See Appendix G for the LAHOS configurations used.

Actual test data requires a slightly more straightforward solution. The RMS values from testing are derived from measurements of pilot input and flight path error. Pilot input measurements are converted to input rates by dividing the change in input by the change in time. These data streams are reduced to RMS values using Equations (19) and (20).

$$\text{RMS } \dot{u} = \sigma_{\dot{u}} = \sqrt{\frac{1}{T} \int_0^T \dot{u}^2 dt} \quad (19)$$

where

$$\text{RMS err} = \sigma_{\text{err}} = \sqrt{\frac{1}{T} \int_0^T y^2 dt} \quad (20)$$

- \dot{u} = Pilot Input Rate (pounds / second)
- err = error
- y = Flight Path Angle Error (degrees)
- T = Time Duration of Measurement (seconds)

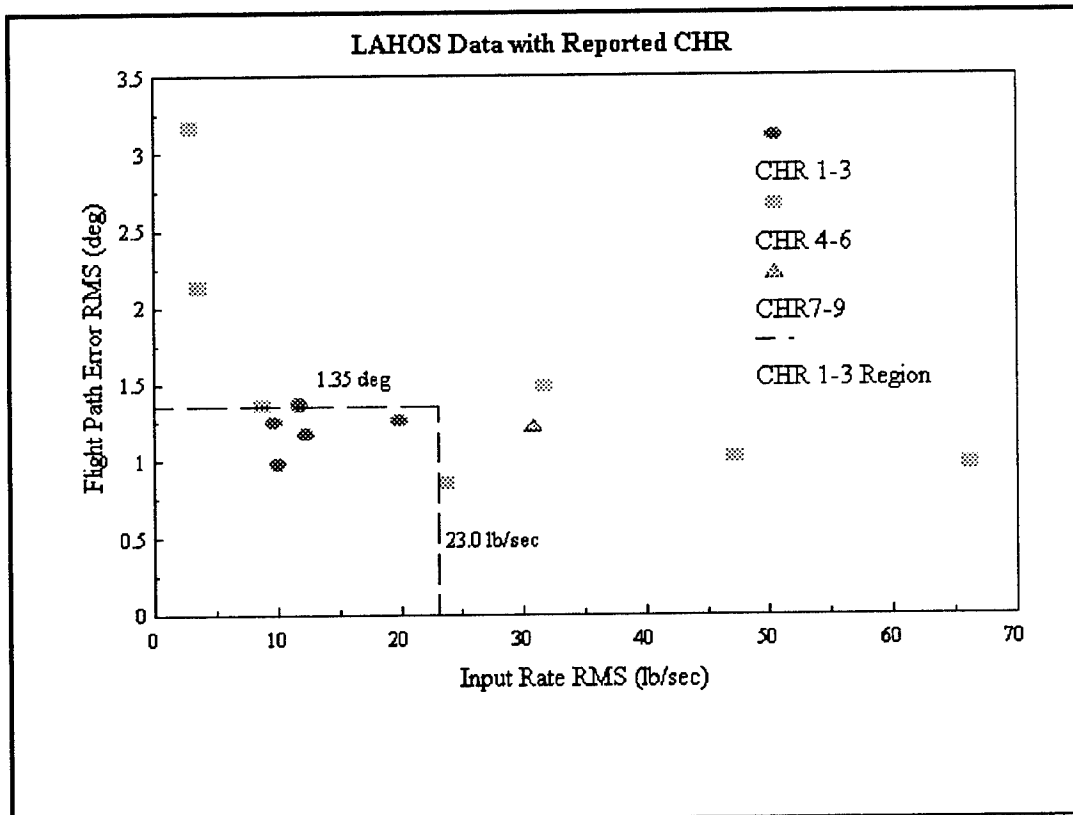


Figure 3.4 LAHOS Database RMS versus Cooper-Harper Ratings (CHR)

Optimal Control Model. A related method of determining handling qualities is with an Optimal Control Model (OCM). This method assumes that the pilot estimates the state of the controlled system and develops a control strategy which minimizes a performance index. The resulting controller consists of a Kalman Bucy Filter (KBF), a linear predictor, and a set of Linear Quadratic Regulator (LQR) gains. See Figure 3.5. For the Systems Technology, Inc. program the LQR is solved to find the desired neuromuscular time constant. Next the Kalman filter is solved to obtain the desired observation noise. From this point the performance index and pilot describing function are calculated. (14:3-13)

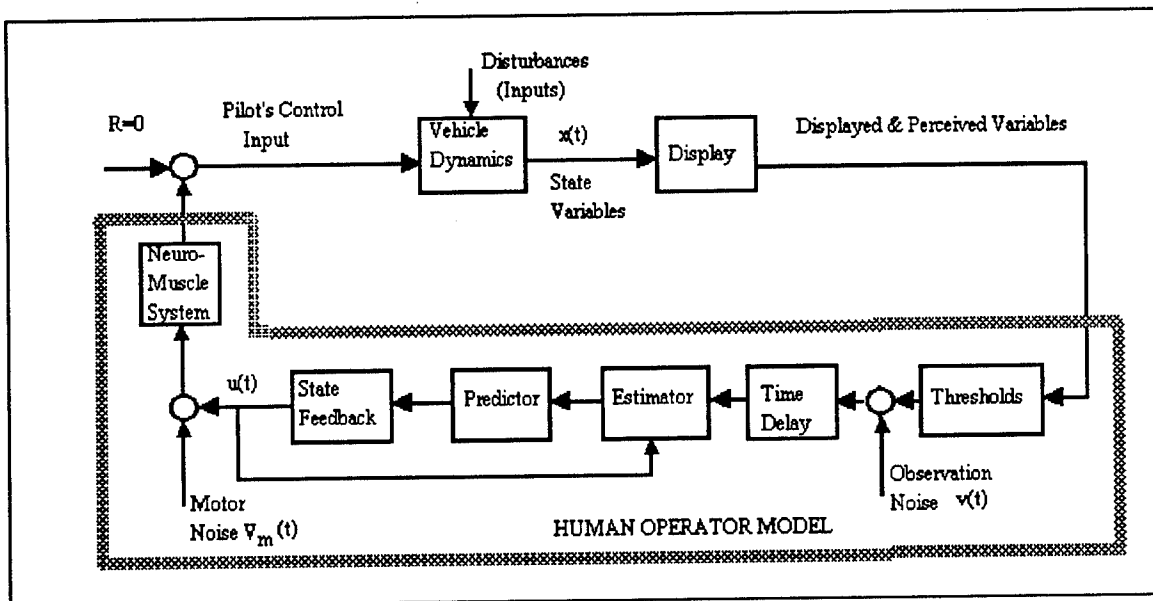


Figure 3.5 Block Diagram Optimal Control Model

The aircraft dynamics are represented by a linear state vector and vector-matrix Equations. For the LQG problem the forcing function is modeled as white Gaussian noise shaped by coloring filters. These disturbances are modeled at the aircraft plant output. This leads to the OCM solution typically being of the order $2n+5$ states,

where n is the number of plant and filter states. (2:Sec 3, 2) Consequently, the aircraft model should be the lowest order suitable to the investigation.

The pilot's visual indifference threshold values are modeled with a Gaussian-input describing function and incorporated into the observation noise. In addition noise is added to each pilot observation to simulate the nonlinear remnant of the pilot as well as his random error in observing displayed variables. The internal delays inherent to the pilot are modeled as a single perceptual delay. (14:11-13) The precise settings used for these noises and delays is found in Appendix A.

The optimal part of this method comes from the LQR minimizing a cost function. That function is equation (21).

$$J = \int_0^{\infty} [x^T(t)Qx(t) + \dot{u}^T(t)R\dot{u}(t)]dt \quad (21)$$

where

- J = Performance Index
- x = State Matrix
- \dot{u} = Control Rate Matrix
- Q = State Weighting Matrix
- R = Control Rate Weighting Matrix

Just as in the RMS method the cost function deals with both performance and workload. The first part of the equation relates to performance and the second half directly relates to workload. Obtaining the minimal performance index denotes the best performance and workload combination. This lowest cost is transformed into a predicted Cooper-Harper rating using equation (22). (14: 52)

$$\text{CHR} = 5.5 + 3.7 * \log_{10}\left(\frac{J}{\sigma_c^2 * \omega_w^2}\right) \quad (22)$$

J = Performance Index

σ_c = RMS of the Forcing Function (radians)

ω_w = Bandwidth of the Forcing Function (radians / second)

IV. Experimental System

The experimental system for the analysis of quickening is a closed-loop command tracking system. The three major components of the system, the display, the pilot, and the aircraft, are all in the forward path. Each of these components will be discussed later in the chapter. Configured as in Figure 4.1, this system is an accepted method of modeling display dynamics. (1:2) Combined with the metrics of chapter III and the use of Single Input Single Output (SISO) transfer functions, this setup is used for analysis and prediction of the aircraft's handling qualities.

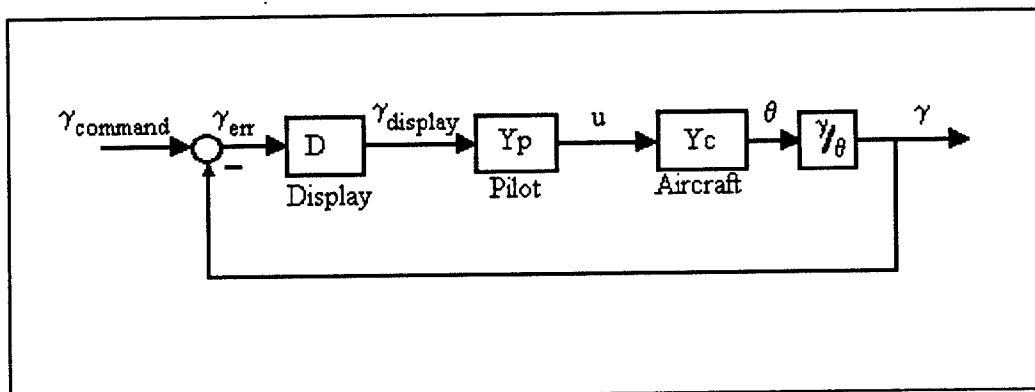


Figure 4.1 Flight Path Tracking System

Display. This block consists of the flight path marker displayed to the pilot. For quickening the pitch angle format discussed in chapter II, Equation (1), is used.

$$QI = G \cos\phi \frac{s}{s + \frac{1}{\tau}} \theta \quad (1)$$

To simplify analysis the bank angle was confined to zero degrees. Theoretically, the gain should be set to one for optimum results. Flight test has shown, however, that 0.7 actually works better for approach and landing. (5:27) Initial investigations show that the optimum time constant with a gain of one remains the same for a gain of 0.7. For time constant analysis, a gain of one is used. As described in chapter II, the quickening is then added to the actual flight path angle and this combination becomes the displayed flight path marker. In the modeled tracking task the transfer function for the display becomes Equation (25).

$$\gamma_{\text{display}} = \gamma_{\text{err}} + G \frac{s}{s + \frac{1}{\tau}} \theta \quad (23)$$

$$\frac{\gamma_{\text{display}}}{\gamma_{\text{err}}} = 1 + G \frac{s}{s + \frac{1}{\tau}} \frac{\theta}{\gamma_{\text{err}}} \quad (24)$$

using θ/γ derived from Equation (12)

$$D = \frac{\gamma_{\text{display}}}{\gamma_{\text{err}}} = 1 + G \frac{s}{(s + \frac{1}{\tau})} \frac{(s + \frac{1}{T_{\theta_2}})}{\frac{1}{T_{\theta_2}}} \quad (25)$$

where

D = Display transfer function with quickening

G = Gain

θ = aircraft pitch angle (degrees)

γ_{err} = aircraft flight path angle error between actual flight path and commanded flight path angle (degrees)

γ_{display} = aircraft flight path angle error displayed on HUD (degrees)

τ = time constant (seconds)

s = Laplace complex frequency variable

The unquickened display is modeled as a direct feed of one for the display transfer function. The aircraft pitch angle is limited to less than 30 degrees so that blending is not a factor for this study.

Pilot. The second major block in the system consists of one of two forms. One was the Neal-Smith criteria pilot model discussed in chapter III. This form is used in conjunction with the Neal-Smith criteria while the second pilot model is an optimal control model (OCM) developed by Systems Technology, Inc.. (14) The optimal control pilot model lends itself to future development to a multiple input multiple output system as well as designing in several human factors pertinent to displays. The drawback of the optimal control model lies in its complexity. Using both types of pilot models allows results verification from different methods. The output of both pilot models is force in pounds for a displayed flight path error input in degrees.

Optimal Control Model. The Systems Technology, Inc OCM program is designed for use with a SISO system. Many variables are selected by the program operator and have an impact on how well the model does. A previous study ran a sensitivity analysis on this particular OCM and developed recommended settings to obtain the best results. (2) These suggested parameter settings are used for the analysis of the system and are found in Appendix A.

Aircraft. The aircraft block consists of a combined aircraft-flight control system transfer function. Using force in pounds as an input the transfer function returns aircraft pitch attitude in degrees. The aircraft aerodynamic model being used for the paper analysis and study is the General Dynamics Variable In-flight Simulator Test Aircraft (VISTA) F-16. Modified from a block 30 F-16D, VISTA had direct force

vertical surfaces and an enlarged dorsal spine. The direct force surface modeling is excluded as a control surface for this study. In all other respects the aerodynamic model for VISTA is sufficiently representative of the F-16. This aerodynamic model is combined with a block 25 F-16 flight control system using standby gains to create the pitch attitude to stick force transfer function. See Appendix B for the aerodynamic models and flight control system.

A low order match to the full order transfer function is then accomplished using a matching subroutine. See Appendix C. This low order match takes the form of a short period approximation and a first order flight control system. Using the low order system aids in the analysis as well as keeping the OCM pilot order to a manageable level. Matching tolerances are those described by Mil-Std-1797A for equivalent systems. (12:682)

Two different flight conditions are explored. The first is a pressure altitude of 1,000 feet and 0.24 Mach number. The second is at the same pressure altitude, but 0.60 Mach number. This spread in Mach number allows an evaluation of the results compared with simulator determined values for the quickening algorithm. The simulator determined values are derived from empirical testing done as outlined in Mil-Std-1787B. (11:Sec A, 10-12)

Flight Path Angle to Pitch Attitude. Although not a major block in the system, the transfer function transformation from pitch angle to flight path angle remains a necessary part. This transformation is the same as described in chapter III, in Equation (12). This transfer function still has the associated limitation, T_q (defined by

Mil-Std-1797A) is not much less than T_{θ_2} , the high frequency pitch attitude zero time constant. This condition is recommended by Mil-Std-1797A. (12:257-258)

$$\frac{\gamma}{\theta} = \frac{\frac{1}{T_{\theta_2}}}{s + \frac{1}{T_{\theta_2}}} \quad (12)$$

With this last block in the system complete, the search for an analytically determined optimum time constant can begin.

V. Quickening Time Constant Analysis

The whole reason for quickening lies in the inherent lag of the actual flight path angle. Behind the use of quickening to rid the flight path marker of this problem is the pilot's preference for instant feedback. During visual flight the pilot gets this feedback from the aircraft pitch attitude. For instrument flight the pilot uses the attitude indicator for feedback. Pilot comments show that the nearly instantaneous reaction of the attitude indicator resulted in a "firm" response to control inputs. This "firmness" caused the pilots to prefer the attitude indicator as a primary flight control reference. (7:3) Based on these observations a desirable quickening time constant should result in a "firm" response. The flight path marker (FPM) should react similar to a pitch attitude indicator or artificial horizon.

With this idea in mind, examine the open loop experimental system without the pilot. Essentially, look at the aircraft dynamics-flight control system combination and the display. Figure 5.1 represents the total open loop aircraft as seen by the pilot. See Equation (26) for this open loop transfer function..

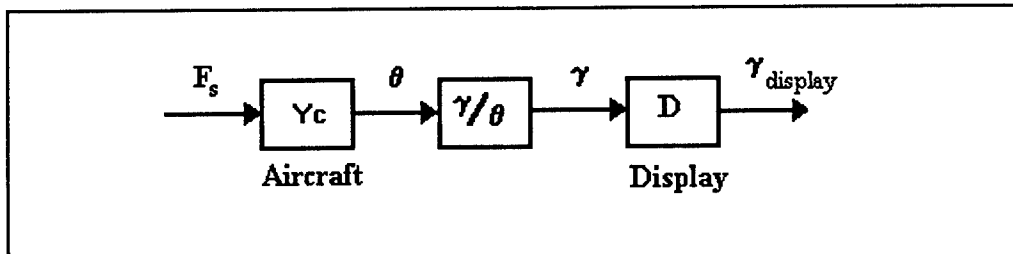


Figure 5.1 System Open Loop Aircraft

$$OL = Y_c (\gamma/\theta) D = \frac{\theta}{F_s} \frac{\gamma}{\theta} (1 + Q \frac{\theta}{\gamma}) \quad (26)$$

where

OL = Open Loop Transfer Function Displayed Flight Path to Stick Force

Y_c = Aircraft Model Transfer Function

γ/θ = Flight Path Angle to Aircraft Pitch Angle Transfer Function

D = Display Transfer Function

θ/F_s = Aircraft Pitch Angle to Stick Force Transfer Function

Q = Pitch Attitude Quickening Filter

Further substitution for the transfer functions yields the total aircraft flight path angle transfer function shown in Equation (28) as seen by the pilot. For the ease of analysis, let the aircraft model transfer function which has a short period approximation be shortened to a generic denominator and the high frequency zero seen in Equation (27).

$$\frac{\theta}{F_s} = \frac{s + \frac{1}{T_{\theta_2}}}{\Delta} \quad (27)$$

and

$$OL = \frac{s + \frac{1}{T_{\theta_2}}}{\Delta} \frac{\frac{1}{T_{\theta_2}}}{s + \frac{1}{T_{\theta_2}}} \left(1 + \frac{s}{s + \frac{1}{\tau}} \frac{s + \frac{1}{T_{\theta_2}}}{\frac{1}{T_{\theta_2}}} \right) \quad (28)$$

where

T_{θ₂} = High Frequency Zero Time Constant

Δ = Generic Short Period Denominator

τ = Quickening Time Constant

If this flight path angle total transfer function can be made to look like the pitch angle to stick force transfer function in Equation (28), the pilot will see a pitch angle type response. The FPM will move with the near instantaneous motion seen on an attitude indicator. This motion should result in the same "firmness" for control response of the FPM as preferred by pilots on the attitude indicator. If the quickening time constant is set to the aircraft dynamic's pitch attitude high frequency zero time constant, $T_{\theta 2}$, the desired result is achieved. The open loop transfer function now becomes Equation (29).

$$OL = \frac{s + \frac{1}{T_{\theta 2}}}{\Delta} \frac{\frac{1}{T_{\theta 2}}}{s + \frac{1}{T_{\theta 2}}} \left(1 + \frac{s}{s + \frac{1}{T_{\theta 2}}} \frac{s + \frac{1}{T_{\theta 2}}}{\frac{1}{T_{\theta 2}}} \right) \quad (29)$$

Which simplifies to Equation (30).

$$OL = \frac{1}{\Delta} \frac{1}{T_{\theta 2}} \left(1 + \frac{s}{\frac{1}{T_{\theta 2}}} \right) \quad (30)$$

By multiplying this Equation out and recombining terms the following results:

$$OL = \frac{1}{\Delta} + \frac{s}{\Delta} = \frac{s + \frac{1}{T_{\theta 2}}}{\Delta} = \frac{\theta}{F_s} \quad (31)$$

As can be seen the consequence of setting $\tau = T_{\theta 2}$ is that the total flight path response becomes a pitch type response with the flight path time lag removed. This desirable

response type is a good indication that setting $\tau = T_{\theta_2}$ is at or near the optimum value for the quickening time constant.

Not only should this be an agreeable solution, but it is a beneficial one as well. The aircraft's pitch attitude dynamics and, hence, the high frequency pitch attitude zero must be known for the flight control system design. The high frequency pitch attitude zero is inversely proportional to the aircraft's lift coefficient, $C_{L\alpha}$. More exactly, T_{θ_2} can be approximated by Equation (32). (12: 186, 259)

$$T_{\theta_2} \doteq \frac{V\alpha}{g n} \doteq \frac{V}{g} \frac{W}{C_{L\alpha} \frac{1}{2} \rho V^2 S} = \frac{2W}{g C_{L\alpha} \rho V S} \quad (32)$$

where

- V = true airspeed (feet / second)
- g = force of gravity (feet / second / second)
- W = aircraft weight (pounds)
- $C_{L\alpha}$ = Lift coefficient
- ρ = density (pounds / feet³)
- S = wing surface area (feet²)
- n = load factor
- α = angle of attack (radians)

All these factors for a flight condition are usually known to the designer. This inverse relationship for T_{θ_2} versus airspeed and density also matches the trend of the scheduling formula of Mil-Std-1787B. This formula as seen in Equation (8) has the quickening time constant being inversely proportional to airspeed and density ratio.

Since the information required for the quickening time constant has to be researched for the flight control system and aircraft dynamics beforehand, no special investigation is required. The quickening time constant becomes a known quantity. Quickening becomes cheaper in terms of money and time invested for

implementation. The next step is verifying this concept as a desirable solution using case studies with the F-16 aircraft model.

VI. F-16 Model Case Study

A realistic aircraft model is used to validate the optimal time constant described in chapter V as measured by the handling quality metrics previously described. These metrics include Neal-Smith criteria, Root Mean Square analysis, and Optimal Control Model analysis. The F-16 model is used in the experimental system described in earlier chapters to evaluate two flight conditions. These flight conditions are at 1,000 feet pressure altitude and 0.24 True Mach number and 0.60 True Mach number. The 0.24 Mach number flight condition will be known as Case One and the 0.60 Mach number as Case Two. A range of time constants is evaluated for these flight conditions to include the high frequency zero time constant ($T_{\theta 2}$), a simulator derived one, and a baseline nonquickened system. See Table 6.1. The simulator derived time constant comes from a previous study using the methods of Mil-Std-1787B to empirically determine the quickening time constant. The range of time constants allows direct comparison with the empirically derived simulator time constant. Additionally, this range should establish that the optimal time constant is near $T_{\theta 2}$.

An interesting fact was discovered during the investigation of the empirically derived F-16 simulator quickening time constants. When the computer code for quickening was implemented in the previous study instead of using the density ratio, ρ / ρ_0 , the simulator implemented the quickening algorithm using the pressure ratio, P / P_0 . The reason for this change is unknown. Conceivably, the pressure ratio was an easier direct in-flight measurement to use than the density ratio. Regardless, the

difference between the two time constant values calculated by the different ratios is not significant for these flight conditions. See Table 6.2. The higher in altitude the aircraft goes the more significant become these differences. For this reason if pressure ratio instead of density ratio is used, the A and B constants in the scheduling formula need to be adjusted accordingly. The simulator values for A and B using pressure ratio are A= -0.725 and B= 385.

Table 6.1
Case Study Quickening Time Constants

Case One	Case Two
0.00 = Nonquickened	0.00 = Nonquickened
0.20	0.15
0.60	0.28 = F-16 Simulator
1.00	0.50
1.66 = T ₀₂	0.77 = T ₀₂
1.80 = F-16 Simulator	1.00
2.00	1.40

Table 6.2.
Case Study
Density Ratio versus Pressure Ratio for Quickening Time Constants

Scheduling Method	Quickening Time Constants	
	Case One	Case Two
Density Ratio, ρ / ρ_0	1.787	0.278
Pressure Ratio, P / P_0	1.876	0.284
Difference	4.98 %	2.16 %

Case One. The first case is a low dynamic pressure situation. The equivalent low order aircraft model is found in equation (33). To obtain a better fit for the low order system, $T_{\theta 2}$ was not fixed during the matching for this one case.

$$Y_c = \frac{2.914(s+0.573)e^{-0.17s}}{s(s+2.787)(s^2+0.856s+17.1)} \quad (33)$$

The high frequency zero time constant, $T_{\theta 2}$, is 1.66 for the original airframe dynamics. The equivalent short period frequency is 4.14 radians per second with a damping ratio of 0.103.

The pilot transfer functions for each of the different display blocks can be found in Appendix D. Both Neal-Smith and Optimal Control Model (OCM) pilot configurations are studied. All the Neal-Smith predictions were for the Controllable category. The OCM pilot for this flight condition gave the most favorable Cooper-Harper Rating (CHR) predictions as seen in Table 6.3.

Table 6.3
Case One
Optimal Control Model Cooper-Harper Predictions

Quickening Time Constant	Cooper-Harper Rating (CHR)
0.00 = Nonquickened	5.79 ≈ 6
0.20	5.08 ≈ 5
0.60	5.60 ≈ 6
1.00	5.57 ≈ 6
1.66 = $T_{\theta 2}$	5.45 ≈ 5
1.80 = F-16 Simulator	5.43 ≈ 5
2.00	5.41 ≈ 5

Root Mean Square (RMS) analysis also predicted an Acceptable level rating for all the configurations. See Figure 6.1. This Acceptable level rating prediction results from the workload required of a minimum of 30 pounds per second. The performance in all cases is good with the highest flight path RMS error being approximately 0.75 degrees. The nonquickened system delivers the least workload, but also has the worst performance. The theoretically optimum time constant gives the best performance at a slightly greater workload. The simulator derived time constant is very close to the theoretical optimum in both performance and workload. The trend with quickening in the display indicates less workload and better performance as the quickening increases up to the theoretical optimum, T_{02} . After this point the workload decreases or gets better, but the performance gets worse. These results conform with theory. The more quickening the better the performance for less work until too much quickening is added and performance deteriorates.

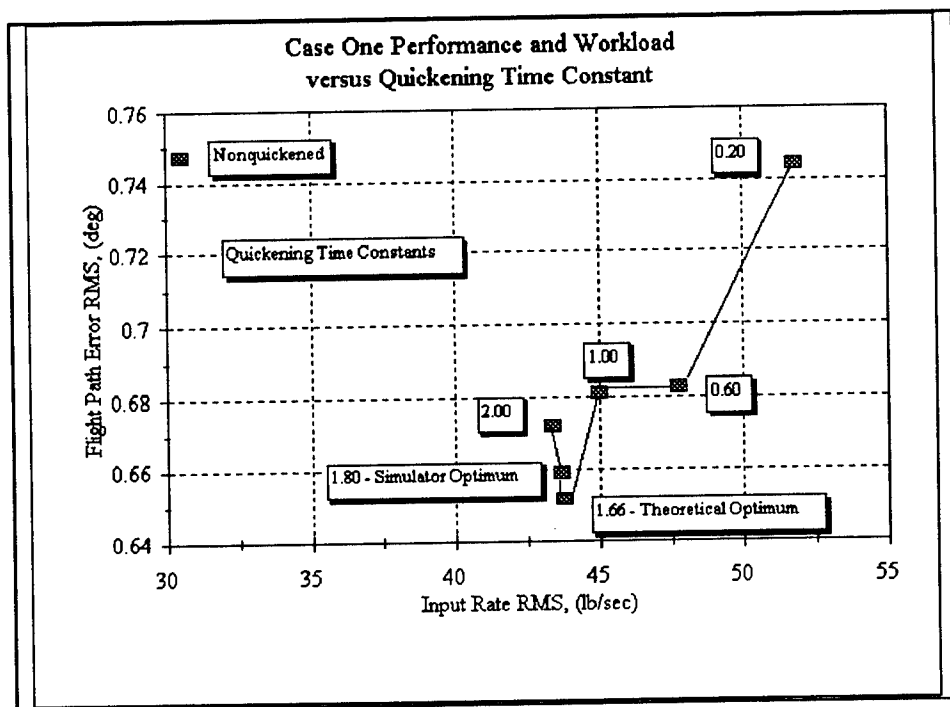


Figure 6.1 Case One Root Mean Square (RMS) Results

The most desirable time constant lies the closest to the origin in Figure 6.1. This assumes that the pilot puts equal weight on both performance and workload for this particular task. While not a perfect assumption at all times, for the paper analysis this assumption is considered adequate. As one can see the theoretical prediction is the closest to the origin. Therefore, for this flight condition the most desirable time constant is $T_{\theta 2}$.

Case Two. The second case is a higher dynamic pressure environment than the first. The aircraft-flight control system pitch attitude to force input yields a lower order equivalent system seen in equation (34).

$$Y_c = \frac{4.032(s+1.299)e^{-0.48s}}{s(s+2.926)(s^2+2.84s+123)} \quad (34)$$

The equivalent short period frequency is 11.09 radians per second with a damping ratio of 0.128. The high frequency zero time constant, $T_{\theta 2}$, for this case is 0.77. The quickening time constants used are in Table 6.1 and the associated pilot transfer functions in Appendix D.

Both OCM and Neal-Smith pilot models are investigated. The Neal-Smith model gives the best results of the two with OCM models being unattainable. The STI OCM program produced error messages on all attempts for this case. The Neal-Smith predictions for the different time constants are found in Table 6.4. As seen the systems are all Satisfactory level with the exception of the two shortest quickening time constants. Note that the simulator derived time constant, 0.28 seconds, produces an Acceptable level. As the quickening increases the handling quality ratings improve.

The interesting part is that the baseline system is also a Satisfactory level and the addition of minimal quickening destabilizes the system.

Table 6.4
Neal-Smith Pilot Rating Predictions

Quickening Time Constants	Neal-Smith Pilot Cooper-Harper Rating Levels
0.15	Unstable
0.28	Acceptable
0.50	Satisfactory
0.77	Satisfactory
1.00	Satisfactory
1.40	Satisfactory
0.00=Nonquickened	Satisfactory

The Root Mean Square analysis predicted much higher workloads for all the systems compared with case one. See Figure 6.2. The workload for quickening of 0.15 seconds takes an infinite amount of input rate since that system is unstable and was not graphed. The best prediction for any of the systems from RMS analysis is an Acceptable level because of the workload. See Appendix E for the exact RMS values. The general trend for workload is the same as for case one. As the amount of quickening increases the workload decreases or improves. This trend holds until the theoretically optimum time constant at which point the workload starts increasing as quickening increases. This workload trend conforms to theory. As in case one, the baseline, nonquickened, system has a lower workload than the quickened systems.

Performance in general conforms with theory. Quickening reduces the flight path error when compared with the baseline system. However, the performance with more quickening got slightly worse as the workload decreased until the theoretical optimum was reached. The theoretically determined time constant is still the most desirable, however, as it is the closest to the origin in Figure 6.2.

Case two differs from case one for the RMS analysis in the performance trend among quickening time constants and most notably in the workload magnitude. One possible reason is the higher dynamic pressure. Since the two flight conditions are at the same altitude the difference consists of airspeed. The case two aircraft flies almost twice as fast as in case one. Case two also represents conditions twice as fast as the aircraft flown in the LAHOS database. Possibly, the second case exceeds the boundaries of usefulness of the LAHOS database. Flight test of the tracking task at the higher airspeed might show that the handling quality regions have higher workload boundaries. This factor seems reasonable since pilot inputs would need to be quicker at the higher airspeeds to track the same flight path. This factor might explain the discrepancy between the Neal-Smith criteria Satisfactory level predictions and the RMS Acceptable level predictions. Most importantly, although the exact handling quality rating may be incorrect using the current database, this does not affect the trend information or relative ranking of the time constants.

The theoretically determined time constant is the most desirable time constant for case two. Root Mean Square analysis showed it to be the most desirable. The Neal-Smith metric predicted an Acceptable level for the simulator derived time constant and a Satisfactory level for the theoretical time constant. The nonquickened

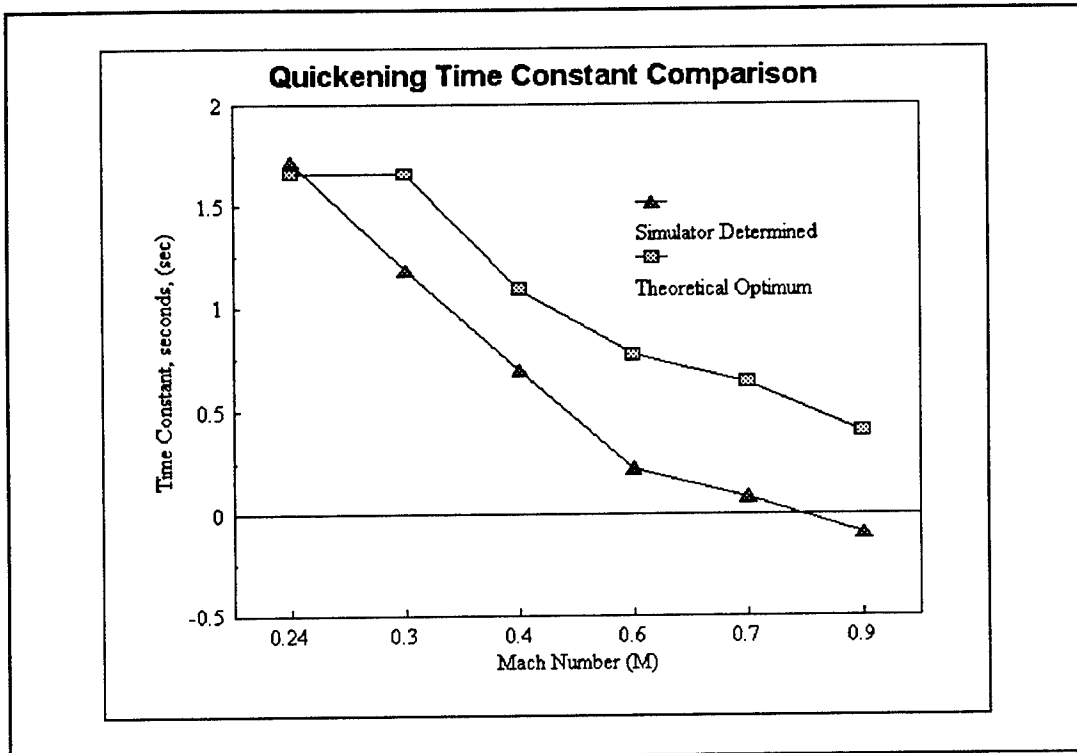


Figure 6.3 Quickening Time Constant Scheduling Curves

baseline system and the theoretical time constant system both predict a Satisfactory level using the Neal-Smith criteria. Based on these results the theoretical time constant is considered the most desirable time constant.

Overall Results. In both case one and two the trends show that the theoretically determined time constant is the most desirable. In each case one pilot model gives consistently better results. For the low dynamic pressure the OCM pilot is preferred and for the high dynamic pressure situation the Neal-Smith pilot model. Throughout the study Neal-Smith pilot models give more believable results and are drastically easier to use. The OCM pilot suffered from being very high order with numerous near pole-zero cancellations to complicate matters. The trends shown by both pilot models are fairly consistent.

Basing the scheduling off the high frequency pitch attitude zero time constant yields a curve that parallels the scheduling of the simulator based time constant. This curve is seen in Figure 6.3. Note that during actual implementation the quickening time constants are limited to values between 0.0 and 2.0. Down to approach speeds, roughly 0.3 Mach number, the correlation between simulator scheduling and $T_{\theta 2}$ is good. There appears, though, to be a bias of approximately +0.5 seconds in the theoretical time constants compared with the simulator scheduling. See Figure 6.4.

At approach speeds, 0.3 Mach number and below, the aircraft dynamics and, therefore, the $T_{\theta 2}$ time constant levels off. This finding is consistent with previous studies showing that for approach and landing the quickening time constant

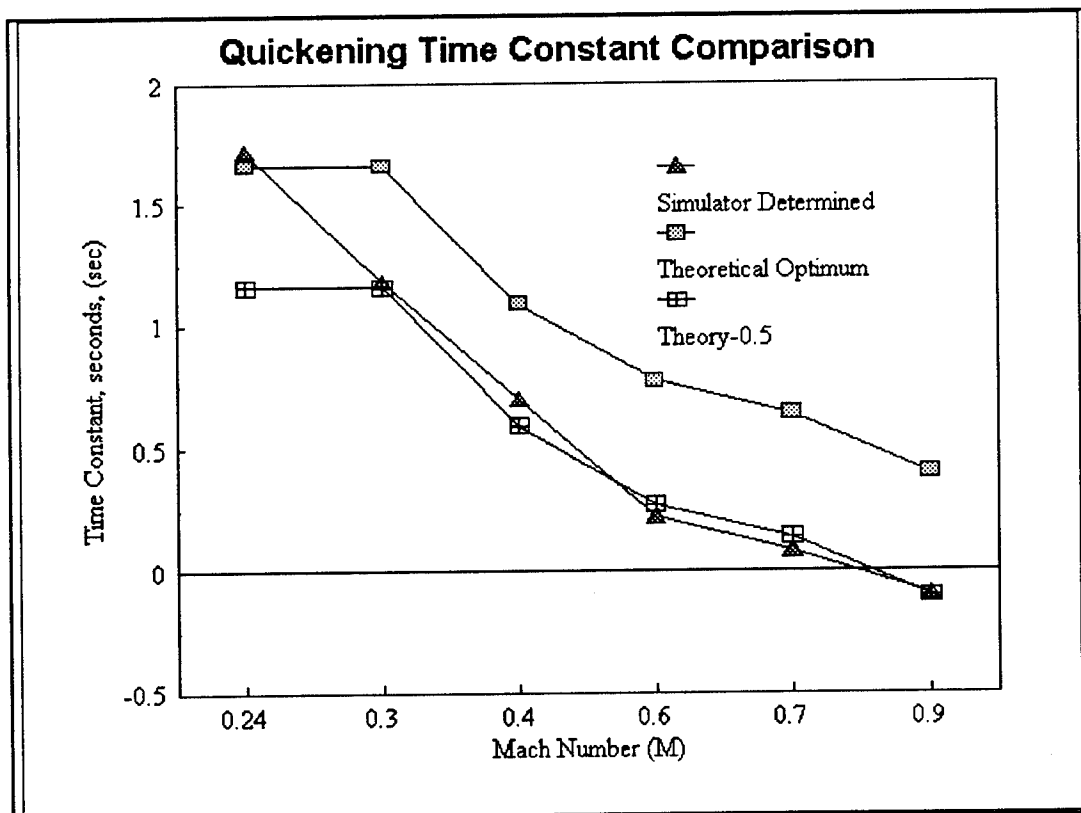


Figure 6.4 Theoretical Optimum Quickening Time Constant Bias

can be fixed. (7:8-7)

The theoretically determined time constant seems to fit as the most desirable time constant. Both flight conditions investigated yield reasonable conclusions that this theoretical approach is the most desirable. Comparison with empirical simulator studies show that the scheduling of the theoretical time constant fits as well, although a slight bias exists. The next step for confirmation is actual flight test.

VII. Flight Test

This chapter presents the results of a flight test evaluation to validate the optimum time constant for the standardized head-up display (HUD) flight path marker (FPM) quickening. This test is the real world verification of the theoretically determined time constant. These test results and the following information are found in AFFTC-TLR-94-83, *A Limited Evaluation of the Optimum Head-Up Display Flight Path Marker Quickening Time Constant for Fighter Type Aircraft in the Low Altitude Arena*. (9) Five time constants were evaluated over the 8.8 hour flight test program from 7 to 11 October 1994 using the CALSPAN Corporation operated NT-33A in-flight simulator.

Test Item Description. The five time constants contained in Table 7.1 were the actual test items being evaluated. Time constant A was the value without quickening or other compensation of the flight path marker. Time constant B was the optimum value determined by the iterative method of MIL-STD-1787B using the ground based F-16 simulator. Time constant C was the theoretically determined time constant presented in chapter V, the airframe pitch transfer function time constant, T_{θ_2} . Time constant D was an empirically derived value to define an upper bound to the optimum time constant. The final time constant, E, was an empirically derived intermediate bound value for data between the optimum quickening and the without quickening point. The exact numerical value of these time constants was flight condition dependent.

Table 7.1
Quickening Time Constants

Configuration/Description	ILS	HUD	Aimoff
A No quickening	0.000	0.000	0.000
B F-16 Simulator determined optimum time constant	1.040	0.087	0.032
C Theoretically determined time constant	1.430	0.699	0.699
D Upper bound time constant to define optimum	1.600	1.200	1.000
E Intermediate bound time constant to define optimum	0.500	0.040	0.010

Once again a bias is noted between the simulator determined time constant and the theoretically determined time constant. For the non-approach configured cases and airspeeds, roughly a 0.63 second bias is present. For the approach configuration the theoretical time constant's value is 0.41 seconds more than the simulator time constant. One possible explanation for the difference is that the simulator time constant depends on the flight control system as well as the aircraft dynamics. The theoretically determined time constant depends only on the airframe dynamics.

The NT-33A (USAF Serial Number 51-4120) was an extensively modified T-33 jet trainer and was used as a three-axis, variable stability, in-flight simulator. The front cockpit of the NT-33A was modified to include a variable feel system, digital and analog fly-by-wire flight control system, and a programmable HUD. The aircraft's computer was capable of artificially producing ILS information to allow the

aircraft to perform ILS approaches at altitude (called an "ILS-in-the-sky"). The evaluation pilot flew in the front seat using the side stick controller and the analog flight control system. The rear cockpit of the NT-33A contained a conventional T-33 flight control system. More information on the NT-33A can be found in *Test Pilot School Flight Syllabus and Background Material for the USAF NT-33A Variable Stability Aircraft* (8).

The electro-hydraulic variable feel system installed in the front cockpit of the NT-33A drove the variable feel sidestick used for the evaluations. The sidestick was a force controller approximating the sidestick controller found in the F-16. An analog stability flight control system was used to alter the NT-33A's inherent stability and control derivatives by means of in-flight adjustable forward path and feedback gains to simulate the flying qualities of a block 25 F-16C/D. The low order equivalent pitch attitude in degrees to force input in pounds transfer function for the aircraft-flight control system are Equations (35) and (36).

$$\Psi_{\chi_{\text{year up}}} = \frac{1.125(\sigma+1.43)e^{-0.254\sigma}}{\sigma(\sigma+2.634)(\sigma^2+3.299\sigma+1.751)} \quad (35)$$

$$\Psi_{\chi_{\text{year down}}} = \frac{11.05(\sigma+0.699)e^{-0.014\sigma}}{\sigma(\sigma+2.989)(\sigma^2+4.151\sigma+3.473)} \quad (36)$$

The Kaiser AVQ-7 Head-Up Display (HUD) located in the front cockpit of the NT-33A was fully programmable and had several display formats that could be selected in-flight. The USAF standard format from MIL-STD-1787B was used. The Mode Control Unit, located in the rear cockpit, allowed push button, manual mode

control and data insertion through interactive format control menus displayed on the HUD.

Test Objectives. The overall objective of the flight testing was to validate the theoretical optimum HUD flight path marker quickening time constant in the longitudinal axis for fighter type aircraft in the low altitude arena. Specific test objectives were to:

1. Qualitatively evaluate the range of time constants listed in Table 7.1 for approach, low level, and weapon delivery phases using pilot comments.
2. Quantitatively evaluate the range of time constants for approach, low level, and weapon delivery phases using Cooper-Harper ratings, RMS error and RMS input rate.
3. Compare theoretical versus test determined optimum time constants.

All test objectives were met by the testing conducted.

Test Procedures. All test points were flown by project pilots from the front seat of the NT-33A aircraft. The NT-33A aircraft's flight control system performance was verified by Calspan personnel to insure it matched F-16C/D flight control system performance. The primary methods of data collection were HUD video and the data acquisition system (DAS).

Aircraft control was relinquished to the safety observer while the evaluation pilot completed his Cooper-Harper rating (CHR). A comment card was also used to provide additional qualitative data and to add support to the Cooper-Harper rating. Three or more different time constants (time and fuel permitting) were evaluated in

succession prior to beginning another task. The desired and adequate criteria used for the evaluations are contained in Appendix F.

On each mission, the pilots evaluated three or more time constants per task. First, the pilots evaluated the time constants in the HUD tracking task. Then they repeated this procedure for the aimoff and ILS tracking tasks. On the second flight, the remaining time constants were evaluated, along with the best time constant from the first flight as determined by pilot comments. In this manner each pilot evaluated all five time constant in each task over the course of two flights. The exact order of the time constants for each pilot was only known by the project engineer and the safety pilot to preserve impartiality. After a pilot had evaluated all five time constants, he filled out a paired comparison questionnaire on the ground to rank order the time constants for each task.

ILS Offset Approach. This task was accomplished in the powered approach (PA) configuration (gear - simulated down, flaps - 30%, speed brake - in). Actual gear extension was not accomplished. Instead, a gear down condition was simulated by changing the flight control laws to the appropriate F-16 gear down control laws. The data band was 7,000 feet pressure altitude (PA) down to 3,000 feet PA or 3,000 feet above ground level (AGL) (whichever was higher). Localizer deflection was maintained within full-scale deflection limits to ensure reliable glideslope information. The airspeed band was plus ten knots to minus five knots of computed final approach airspeed (based on fuel weight).

Once the aircraft was properly configured and on conditions, the safety observer called "begin maneuver," and activated the HUD ILS display. The pilot

followed the localizer steering cues using either the HUD or HSI to align the aircraft on localizer course. Once established on localizer course, the pilot maintained altitude and approached the glideslope from below. The pilot continued to maintain level flight and fly through the glideslope until reaching one dot above glideslope as indicated on the HUD. At one dot above glideslope, the pilot aggressively maneuvered to recapture glideslope using the flight path marker. The pilot attempted to recapture glideslope as fast as possible within five seconds. The pilot minimized power adjustments during the recapture task while maintaining airspeed. HUD displayed ILS raw data was used to provide feedback to the pilot regarding glideslope position. Primary emphasis was on evaluation of the longitudinal response of the FPM. Glideslope control was not to be sacrificed for localizer control. After descending 1,000 feet PA from the entry altitude, the pilot aggressively recaptured level flight and maintained altitude until one dot above glideslope as indicated by the HUD. He then repeated the above procedure for recapturing and tracking the glideslope until reaching decision height at which time the pilot again attempted to aggressively capture level flight using the FPM.

Low Altitude Flight Path Tracking. This task was accomplished in the clean configuration (gear/flaps - up, speed brake - in). The altitude data band was 7,000 feet PA down to 3,000 feet PA or 3,000 feet AGL (whichever was higher). The airspeed band was 280-320 knots indicated airspeed (KIAS). During the maneuver, the safety observer adjusted power to maintain airspeed within the data band.

Once the aircraft was properly configured and on conditions, the safety observer called "begin maneuver," and activated the HUD tracking task. The program

continued for a minimum of 90 seconds. See Figure 7.1 for the tracking program profile. The pilot attempted to aggressively maintain the FPM on the HUD pitch command bar as it randomly moved about the HUD. Only movement in the longitudinal axis was evaluated.

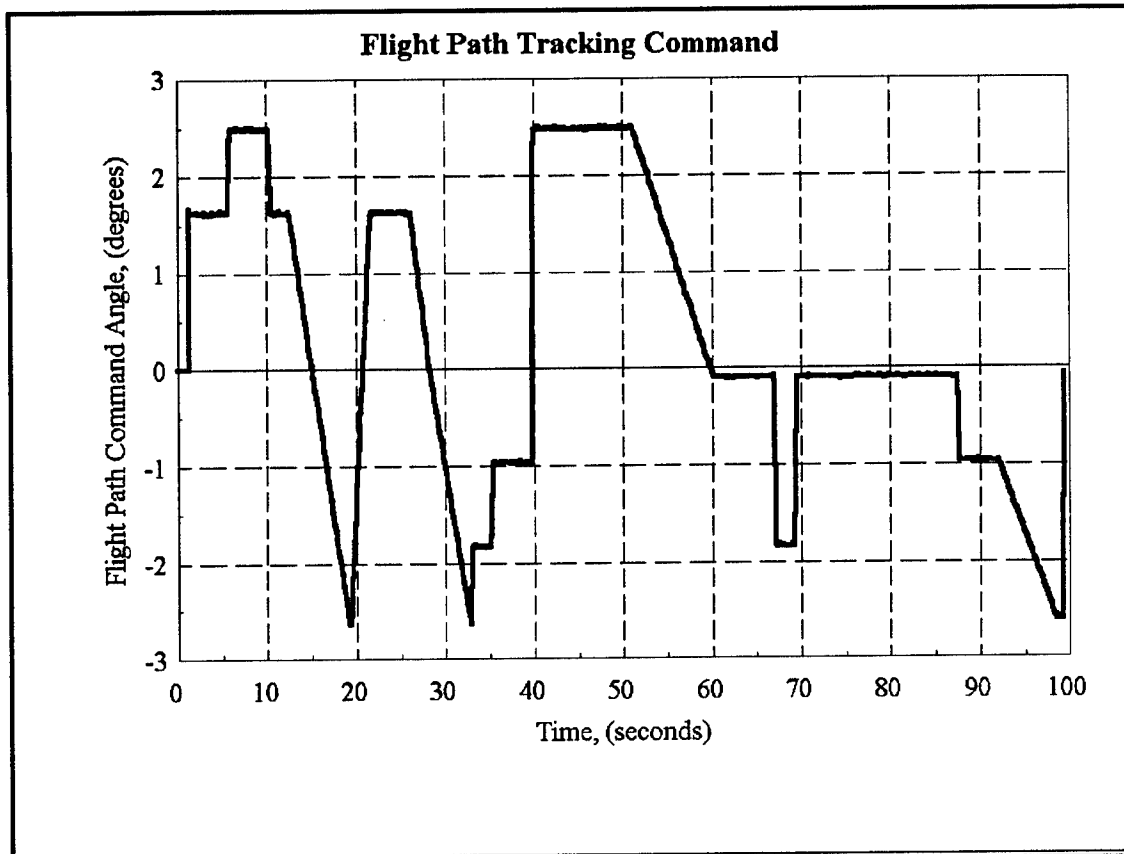


Figure 7.1 Heads-Up Display Tracking Task Command

Aim-off Point Tracking. This task was accomplished in the clean configuration (gear/flaps - up, speed brake - in). The altitude data band was 7,000 feet PA down to 3,000 feet PA or 3,000 feet AGL (whichever was higher). The airspeed band was 250-350 knots indicated airspeed (KIAS).

Once the aircraft was properly configured and on conditions, the safety observer called "begin maneuver." The pilot established a 20 degree dive angle, +/-5 degrees, and maintained trim power setting which resulted in an operationally representative increase in airspeed. Dive angle was established by approaching the target head on, and then executing a 0.2g "bunt" until the desired dive angle was reached. The pilot attempted to aggressively track a prominent stationary ground target with the FPM until maneuver termination. The maneuver terminated as soon as one of the following conditions was met: the pilot had seen enough for a proper evaluation; 3,000 feet AGL was reached; 350 KIAS was reached. Only movement in the longitudinal axis was evaluated.

Data Processing, Reduction, and Analysis. Data collection was both qualitative and quantitative. Quantitative measures of performance consisted of root mean square (RMS) flight path angle deviations from the desired flight path angle as measured by the data acquisition system. Workload was quantitatively defined as RMS measurements of the stick force input rate from the DAS. Further quantitative data were collected as Cooper-Harper ratings and paired comparisons for the three tasks being evaluated. Pilots performed paired comparisons for the different time constants on each task after evaluating all five time constants, in order to rank the various quickening time constants. Paired comparison uses surveys for the subject to make a subjective comparison between an item's performance. The comparison levels are assigned numeric values and then standardized. See Standardized Head-Up Display Symbology Evaluation for reduction methodology of paired-comparisons. The output is a numeric value ranking of the compared items. (15) Qualitative data were

gathered through pilot comments for each event. Pilot comments and Cooper-Harper ratings were assigned in-flight and recorded on both the HUD video and audio tapes.

Test Results. All test objectives were met. Qualitatively and quantitatively, the F-16 ground based simulator derived time constant was preferred to the theoretically determined time constant, although they both gave comparable results. Within the limited scope of this test, flight path marker (FPM) quickening was found to be useful and performance enhancing especially for gross acquisition.

The HUD tracking task was considerably more discerning than the other two tasks with the aimoff tracking being a distant second and the ILS third. For both the aimoff tracking and ILS tasks, the greatest testing value was obtained from the gross acquisition portion of the task and the fine tracking portion was a "non-event." This explains why the HUD tracking was so illuminating--it was basically a constant gross acquisition task. The "ILS-in-the-sky" feature of the NT-33A did not provide enough disturbance to highlight differences in the quickening, even when artificial wind gusts were introduced. Without disturbances such as wind gust, shear, and turbulence, quickening was not observable once the glideslope was established. During steady state conditions such as established on glideslope quickening dies out and no longer affects the FPM. Without disturbances to offset the aircraft from the glideslope there was no change to steady state flight path. The pilots said that the actual ILS approaches flown in the F-16 practice sorties required them to fly much tighter "in-the-loop." Recommend using an actual ILS approach task instead of the NT-33A "ILS-in-the-sky" task for future testing.

A summary of the time constant rankings for each task and by each analysis method follows in Table 7.2. Ordering the time constants using Cooper-Harper ratings (CHRs) was done by comparing the overall grouping of the CHRs for each time constant with pilot comments used to resolve ties. Ordering using root-mean square (RMS) data was done by combining the performance (error RMS) and workload (stick input rate RMS) results with engineering judgement used to resolve ties. Paired comparison results are in Table 7.5 with the more negative the numeric rating, the better liked the time constant..

Cooper-Harper ratings are listed in Table 7.3, the RMS summaries are listed in Table 7.4 and Figure 7.2 through Figure 7.4, and the overall paired comparisons are in Table 7.5. Handling quality RMS regions were determined by using the RMS data and CHRs from this test. See Appendix H. There was some scatter in the data for the CHRs and the RMS results. The individual paired comparisons were extremely scattered. However, the overall paired comparisons were fairly consistent and followed the trends identified by the RMS and CHR results. Because of the small sample size (three pilots), the statistical confidence bounds were of limited utility. If there were a larger sample size, then better confidence intervals could be obtained.

Table 7.2
 Rank Ordered Time Constant Summary
 Best (Top) to Worst (Bottom)

Task	Cooper-Harper Rating	Root Mean Square	Paired Comparison
HUD Tracking	B	B	B
	C	C	C
	E	E	E
	D	A	D
	A	D	A
Aimoff Point Tracking	B	B	B
	C	C	E
	E	E	C
	A	A	A
	D	D	D
ILS Tracking	B	B	B
	C	C	C
	D	D	E
	E	A	D
	A	E	A

A: No quickening
 B: Simulator determined optimum
 C: Theoretically determined
 D: Upper bound value of quickening
 E: Intermediate bound value of quickening

Table 7.3
Cooper-Harper Ratings Summary

	A No Quickening	B Simulator Determined	C Theoretically Determined	D Maximum Value	E Intermediate Value
HUD	3 ¹ 4,6 ² 5 ³	2.5,4 2,3 2,2	4,4.5 2,2 3,3	5 5,4 3	5 2 4
AIMOFF	2 4 2,3	1,2 2,3 1,3	1,3 1,2 3	4 5 4.5	4 2 2,2
ILS	3 5 5	2 2,2 2,5	2 2,2.5 3,1	3 5 2	3 5 2

- ¹ The first row is Pilot A, F-15 background
² The second row is Pilot B, B-52 background
³ The third row is Pilot C, F-16 background

Table 7.4
Root Mean Square Analysis Group Summary

Configuration/ Description	Time Const.	HUD Error (deg)	HUD Work- load (lbs/sec)	ILS Error (deg)	ILS Work- load (lbs/ sec)	Aimoff Error (deg)	Aim- off Work -load (lbs/ sec)
A No Quickening	0.00	0.679	53.7	2.84	40.9	1.43	55.2
B Simulator determined optimum	0.87	0.640	47.1	2.62	43.7	0.68	54.9
C Theoretically determined	0.70	0.668	54.2	2.64	47.2	1.06	49.5
D Upper bound time constant	1.20	0.725	48.5	2.80	43.4	1.63	60.7
E Intermediate bound time constant	0.04	0.631	56.5	3.21	41.7	0.94	51.7

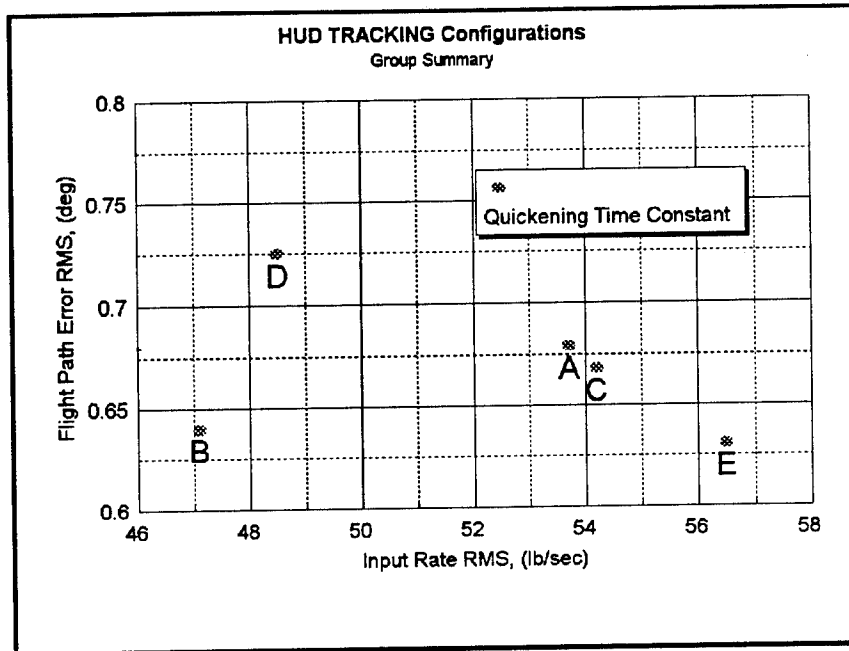


Figure 7.2 HUD Tracking Root Mean Square (RMS) Summary

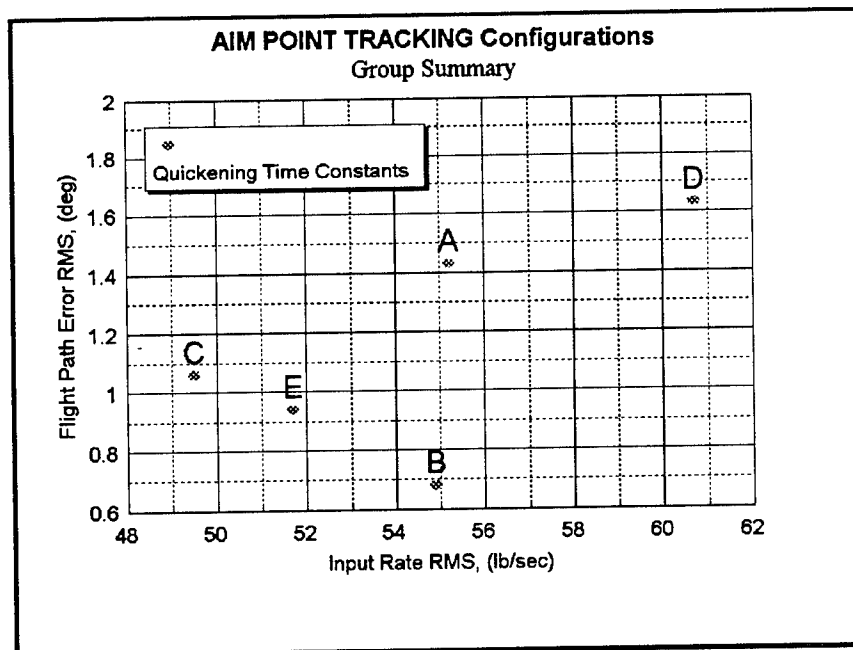


Figure 7.3 Aim Point Tracking Root Mean Square (RMS) Summary

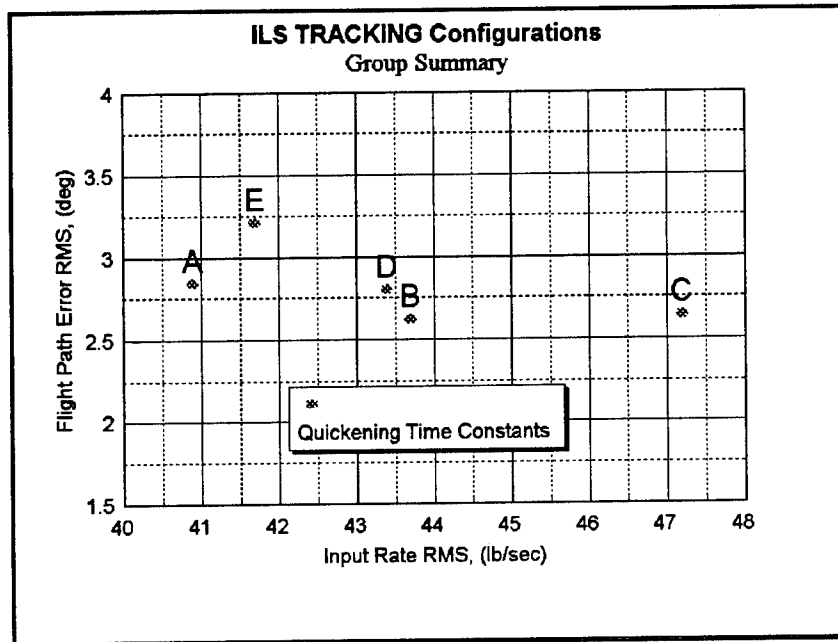


Figure 7.4 ILS Tracking Root Mean Square (RMS) Summary

Table 7.5
Rank Ordered Overall
Paired Comparison Results

HUD Tracking		Aimoff Tracking		ILS Tracking	
Average	Configuration ¹	Average	Configuration	Average	Configuration
-1.70	B	-1.27	B	-3.48	B
-0.81	C	-0.95	E	-1.79	C
0.34	E	-0.45	C	0.99	E
0.40	D	-0.08	A	2.06	D
1.77	A	2.97	D	2.07	A

¹ Configurations are as follows:

- A: No quickening
- B: Simulator determined optimum
- C: Theoretically determined
- D: Upper bound value of quickening
- E: Intermediate bound value of quickening

Some FPM quickening was better than none at all. While there was scatter in the CHR data, some quickening (time constants B and C) generally resulted in a better CHR than no quickening at all (time constant A). The results regarded as most accurate were pilot comments and CHR. Pilot comments were that the workload was lower for the quickened FPM than the unquickened for a given performance level. The HUD tracking root mean square (RMS) results from Table 7.4 bear this out. The unquickened FPM had a larger RMS error and a higher workload than the simulator determined quickening time constant. The pilots commented that quickening increased the predictability of the FPM while reducing the number of overshoots. The paired comparison data clearly showed a preference for quickening with the unquickened FPM consistently rated in the bottom two time constants. The more negative the standardized step number in the paired comparison, the greater preference the pilot had for the time constant. Based on these findings use quickening in the flight path marker.

The ground simulator derived time constant was determined to be the optimum time constant for this evaluation. It was rated the best by a large margin for each task in the paired comparison data. In the HUD tracking task, it had the lowest workload of any of the time constants and achieved the second lowest RMS error. This was somewhat surprising because the test team expected to find the theoretically derived time constant to be the optimum. Pilots commented that the theoretically determined time constant's response was a little too abrupt. In the HUD tracking RMS data, the theoretical time constant achieved comparable performance with the ground simulator time constant, but at quite a bit higher workload. In the paired comparison data, the

theoretical time constant was rated second best for the HUD and ILS tasks and third for the aimoff tracking. Interestingly, the CHR data showed that while the simulator time constant was preferred to the theoretical one, the CHRs were the same level and almost always within a point of each other. Therefore while the theoretical time constant was not the actual optimum time constant, it was a close second and gave comparable results. Use the theoretical time constant as a first estimate of the optimum time constant in the iterative design process.

The close performance and preference of the theoretical and ground simulator time constants was important because the theoretical time constant was determined from the aircraft's pitch transfer function $T_{\theta 2}$, whereas the ground simulator time constant was determined by a lengthy iterative process with pilots flying a simulator. The advantage of the theoretical time constant was that $T_{\theta 2}$ was known by the designer before flight, without the additional lengthy investigation required by the iterative method. For less effort and expense the theoretical time constant delivered comparable performance. The theoretical time constant appears to be an adequate, less expensive substitute for the optimal time constant.

Flight Test Conclusions and Recommendations. Valid data were obtained from flight testing the five different quickening time constants. The three different tasks (ILS tracking, HUD tracking, and aimoff point tracking) gave similar results. Of the three tasks the HUD tracking was the best discriminator between the time constants. Some quickening was preferred to no quickening. The best time constants was the F-16 ground simulator derived time constant closely followed by the theoretical time constant.

The theoretical time constant was not the actual optimum time constant, however it was a close second and gave comparable results. This indicates that the theoretical time constant is an excellent starting point for the iterative design process. Recommend using the theoretical time constant as a first estimate of the optimum time constant in the iterative design process. If resources are not available for this process use the theoretical time constant as an adequate, less expensive substitute for the optimal time constant.

For all the tasks evaluated and for each method of data analysis, flight path marker quickening gave superior results with lower workload when compared with no quickening. Therefore, use quickening in the flight path marker.

Of the three tasks the ILS tracking task was the least discerning between time constants. The lack of disturbances in the NT-33A "ILS-in-the-sky" reduced the quickening seen since quickening dies out at steady state conditions. Addition of turbulence, wind gusts, and wind shear such as seen during an actual ILS would provide better opportunities to evaluate quickening. Use an actual ILS approach task instead of the NT-33A "ILS-in-the-sky" task for future testing.

VIII. Findings and Conclusions

Analysis of the closed loop display augmented system reveals that the optimal solution should be near the high frequency zero time constant, $T_{\theta 2}$. The Optimal Control Model (OCM) and Neal-Smith pilot models along with a short period style low order equivalent system provide the basis to reach this finding which depends on two major assumptions. First, the aircraft is subject to the design considerations noted in Mil-Std-1797A that T_q is not much less than $T_{\theta 2}$. Second, the pilot wants a "firm" response to his control inputs from the flight path marker. Given these assumptions the modeled system leads to the use of the pitch attitude high frequency zero time constant as the theoretically most desirable quickening time constant.

The two case studies using the F-16 aircraft plant investigated the theoretical determined time constant at the flight conditions of 1,000 feet pressure altitude and Mach numbers 0.24 and 0.60. Seven time constants including a F-16 empirically derived one are used to confirm the theoretically determined as the most desirable. Yardsticks for measuring the changes in the system are Neal-Smith criteria, Root Mean Square analysis, and the OCM method. Among these methods use of the Neal-Smith pilot model yields similar results with less complexity in most instances.

Results from the case studies reinforces selection of the theoretically determined time constant, $T_{\theta 2}$. In all cases the theoretical time constant is closest to the origin denoting least workload for suitable performance, the most desirable

position, for the RMS analysis. Both Neal-Smith and OCM methods yield similar results favoring the theoretically determined quickening time constant.

Proceeding on to flight test allows the theory to be put to a practical test. Five time constants were investigated in three different tasks using three different evaluation pilots. Measuring the outcomes both qualitatively and quantitatively yielded consistent results. The F-16 empirically derived simulator time constant was favored over the theoretically determined time constant. A possible reason for this outcome may lie in using the low order equivalent system approximations. Pilots found the theoretically quickened display to be a little too responsive. Yet, the theoretically determined one produced very similar performance and workload compared to the true optimum in each task.

Examining the scheduling of the time constants allows an additional comparison. The theoretical time constant, T_{θ_2} , is inversely proportional to the airframe lift curve slope coefficient, $C_{L\alpha}$, true airspeed, and density. The current scheduling from Mil-Std-1787B depends on air density and true airspeed. For the analytical case studies there is a roughly +0.5 second bias in the theoretical time constant compared with the simulator determined one for flight above 0.3 Mach number. Flight test showed the same bias only with an approximately +0.63 second value for nonapproach conditions. This bias is not as consistent for approach and landing speeds.

This investigation points towards several areas of further study. The most obvious is the use of full order models to discover the reason for the bias between the empirical and theoretical time constants and if it is aircraft dependent. Next comes the

expansion of the current study to include the pitch rate washout filter to confirm that the theory holds for that quickening time constant. Other areas to explore include study of quickening implementation on large aircraft due to their large center of gravity shifts and lateral axis handling qualities for the theoretically determined time constant.

Based on the flight test findings the pitch attitude high frequency zero time constant, T_{θ_2} , is not the optimal quickening time constant. Although the theory is supported by analytical methods, real world implementation shows the theory is not a true optimum. The theoretical method does, however, produce a desirable time constant. This time constant exhibits comparable performance versus the true optimum in actual flight test. Unless the time and money are available to follow the empirical method of Mil-Std-1787B, use of T_{θ_2} as the quickening time constant is recommended. Possible enhancement to the theoretically determined time constant could include subtracting the apparent bias at speeds greater than 0.3 Mach number. The high frequency zero time constant is already a known quantity from testing required for previous aircraft and flight control design. As a minimum, the theoretically determined time constant should be used as a starting point for the iterative design process of Mil-Std-1787B.

Appendix A
Optimal Control Model Parameters

Recommended Pilot Optimal Control Model Settings

Forcing Function Filter
Injected at Plant Output:

$$Y_w = \frac{\sqrt{2}}{6.25s^2 + 3.54s + 1} \quad (37)$$

Intensity of the Driving Noise (V_w)		1
Neuromuscular Time Constant (τ_n)		0.08
State Deviation Weighting (q)		1
Pilot Delay (τ)		0.2
Desired Observation and Motor Noise Ratios		
(ρ_{y1})		-20 dB
(ρ_{y2})		-20 dB
(ρ_{um})		-20 dB
Visual Indifference Thresholds		
(T_{y1})		0
(T_{y2})		0
Fractional Attention Parameter (f)		1
Convergence Threshold	Noises: 0.1	g: 0.001
Initial Guess	Noises: 1	g: 0.1

Information from reference 2, page 3-23

Appendix B
F-16 Case Models

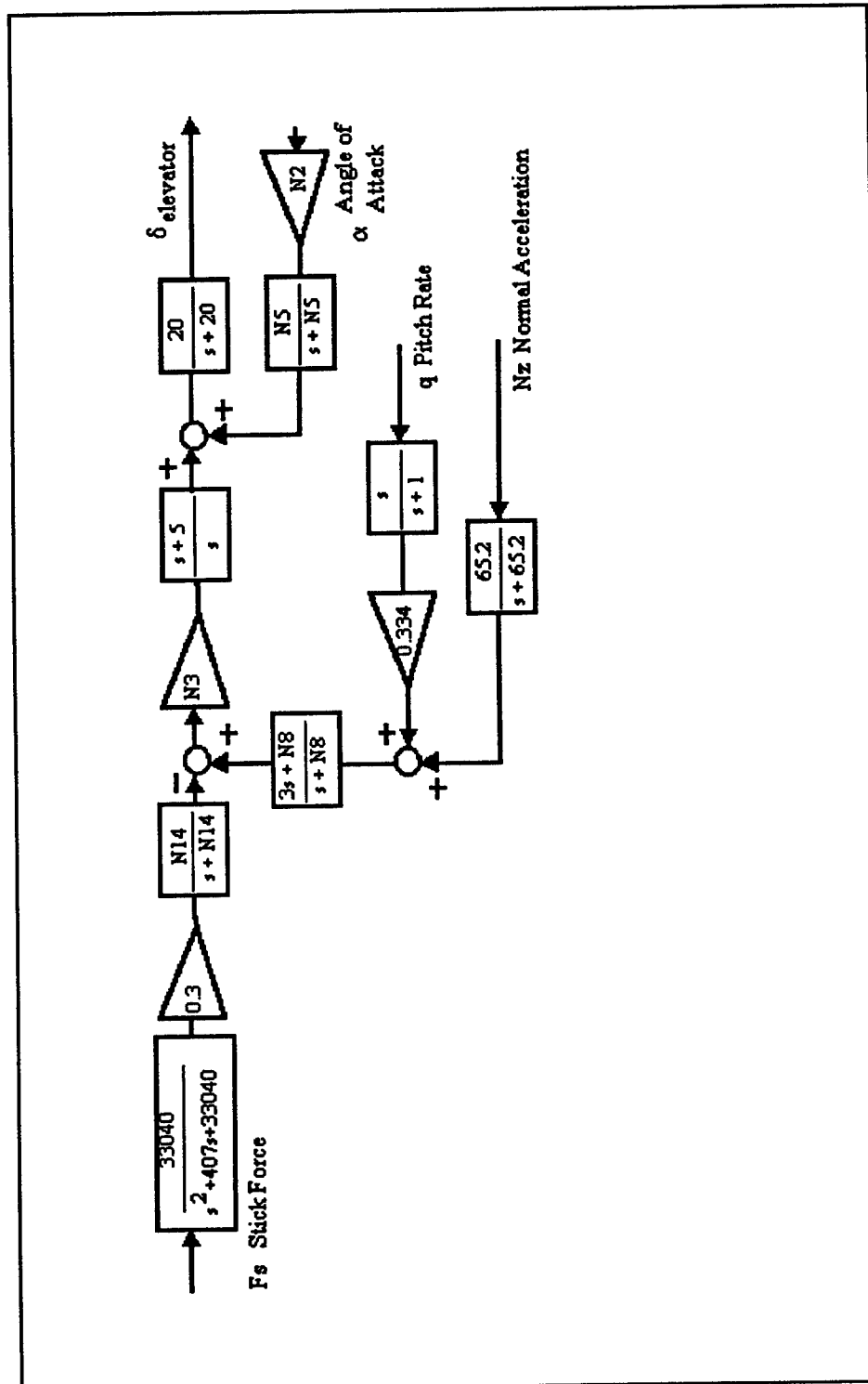


Figure B.1 F-16 Longitudinal Flight Control System

Flight Control System Matlab® M-Files

```
% plantsup.m   Constructs C and D matrices for F-16 aero model
%               use after plantxxxx.m file

%aldot=[ZTHETA ZU ZA ZQ zeros(1,4)];
%qdot=[MTHETA MU MA MQ zeros(1,4)];
%NZ=(1/32.2)*(1/57.3)*(U*(aldot-[0 0 0 1 zeros(1,4)])-13.95*qdot);

C_VISTA=[1 zeros(1,7);           % theta (deg)  1 0 -1 zeros(1,5);           %
gamma (deg)
          0 0 1 zeros(1,5);       % alpha (deg)
          0 0 0 1 zeros(1,4)];    % q (deg/sec)

D_VISTA=[zeros(3,5)];

[A_VISTA,B_VISTA,C_VISTA,D_VISTA]=minreal(A_VISTA,B_VISTA,C_VISTA,D
_VISTA,.0005);

% Standby Gains (good especially for approach type flt)
N2=.42;
N3=1.28;
N5=10;
N8=8.75;
N14=8.3;

[num,den]=ss2tf(A_VISTA,B_VISTA,C_VISTA,D_VISTA,[1;0;0;0;0]);
alphan=num(2,:);
alphad=den;

qn=num(3,:);
qn(1,max(size(qn)))=0;
qd=den;

Nz1=U*(conv([1 0],alphan)-[0 qn]);
Nz2=13.95*conv(qn,[1 0]);
[Nz1,Nz2]=addcon(Nz1,Nz2);
Nzn=(-1/32.2)*(Nz1-Nz2);
Nzd=den;

thetan=num(1,:);
thetad=den;
```

```

% f16theta.m - Forms Transfer function of Theta/Fs for F-16 given
%               control constants and airframe dynamics
%
% Provide  N2,N3,N5,N8,N14
%          alphan,alphad - alpha/del elevator
%          qn,qd - q/del elevator
%          Nzn,Nzd - Nz/del elevator
%          thetan,thetad - theta/del elevator
G1n=33040*.3*N14;
G1d=conv([1 N14],[1 407 33040]);

[innern,innerd]=feedback(20,[1 20],N5*N2*alphan,conv([1 N5],alphad),+1);
[innernm,innerdm]=minreal(innern,innerd);

[middlen,middled]=feedback(N3*conv([1 5],innernm),conv([1
0],innerdm),conv(qn,conv([1 0],[3 N8]))*.334,conv(qd,conv([1 1],[1 N8])),+1);
[middlenm,middledm]=minreal(middlen,middled);

[outern,outerd]=feedback(middlenm,middledm,conv([3 N8],Nzn)*65.2,conv([1
N8],conv([1 65.2],Nzd)),+1);
[outernm,outerdm]=minreal(outern,outerd);

Thetafsn=conv(-G1n,conv(outernm,qn));
Thetafsd=conv(G1d,conv(outerdm,qd));

[Thetafsnm,Thetafsdm]=minreal(Thetafsn,Thetafsd,.15);

```

Case One

VISTA F-16 Aero Model Matlab® M-File

plant0124.m

```
%//  
%// File: model0124  
%// Created: 24-May-93 12:50:53  
%//  
%// Function:  
%// This is a MATRIXx macro file which generates a linear  
%// model in state space form of the F-16 VISTA. The file was  
%// generated by the SRF VISTA simulation.  
%//  
%// Note: Set the MXFILE input parameter from TAE when running  
%// VISTA, to generate this file.  
%//  
%//  
%// *** Flight Condition:  
%//  
%// MACH = 0.2400000E+00 ALTITUDE = 0.1000000E+04 LOAD FACTOR =  
1.0  
%// VELOCITY (ft/sec) = 0.2589626E+03  
%// Wings empty (gear up)  
%// VISTA w/AIM-9Ls  
%//  
MACH = 0.2400000E+00;  
ALTITUDE = 0.1000000E+04;  
U = 0.2589626E+03;  
%//  
%// *** Mass Properties:  
%//  
%// WEIGHT = 0.2489260E+00 VPDOT = -0.5274807E-02 THRUST =  
0.4377627E+04  
%// IXX = 0.9466000E+04 IYY = 0.5902100E+05 IZZ = 0.6606500E+05  
%// IXZ = 0.3850000E+03 X CG = 0.3747000E+02 Z CG = 0.9400000E+02  
%// MAC = 0.1132000E+02 AREA = 0.3000000E+03 SPAN =  
0.3000000E+02  
%//  
%//  
%// *** Trim Solution:  
%//  
%// ALPHA = 0.1421472E+02 ELEV = -0.9321508E+00 TEF =  
%// LEF = 0.2500000E+02 QBAR = 0.8228021E+02 CLQ = 0.9965092E+00
```

%// CMS = -0.3052126E-01 CDQ = 0.1720819E+00

%//

ALPHA = 0.1421472E+02;

ELEV = -0.9321508E+00;

QBAR = 0.8228021E+02;

CLA = 7.4387E-02;

%//

%// *** Longitudinal non-dimensional aero derivatives - stability axis:

%// positional units = 1/degrees, rate units = 1/radians

%//

%//	Cm	CL	CD
%// ALPHA (DEG)	4.0686E-03	7.4387E-02	2.2778E-02
%// ELEVATOR (DEG)	-9.6737E-03	1.1998E-02	2.2680E-03
%// T.E. FLAP (DEG)	4.9411E-04	5.3525E-03	1.7136E-03
%// Q (RAD)	-5.7191E+00	4.3436E-01	8.3412E-02
%// ALPHA DOT (RAD)	-1.0582E-01	-7.5507E-01	0.0000E+00
%// U (VEL-FT/S)	-1.2138E-05	-7.8678E-05	3.0473E-05

%//

%// *** Lateral-directional non-dimensional aero derivatives:

%// positional units = 1/degrees, rate units = 1/radians

%//

%//	Cn	Cl	CY
%// BETA (DEG)	3.7176E-03	-2.6754E-03	-1.7790E-02
%// P (RAD)	-1.1136E-01	-3.4008E-01	2.1267E-01
%// R (RAD)	-5.2412E-01	-3.7125E-03	6.4125E-01
%// RUDDER (DEG)	-1.4471E-03	2.8806E-05	3.4828E-03
%// FLAPERON (DEG)	4.8903E-04	-2.0790E-03	2.2672E-04
%// DIFF TAIL (DEG)	-6.5073E-04	-1.6392E-03	2.5224E-03

%//

%// *** Load coefficients:

%//

ZA = -0.583872 ;

MA = 1.00505 ;

XA = 25.6644 ;

ZDE = -0.861032E-01;

MDE = -2.62313 ;

XDE = 1.36802 ;

ZDF = -0.396283E-01;

MDF = 0.134451 ;

XDF = -0.634507 ;

ZQ = 0.998865 ;

MQ = -0.602391 ;

XQ = -64.1725 ;

ZU = -0.419285E-03;

MU = -0.212406E-02;

```

XU = -0.529722E-02;
ZTHETA = -.305331E-01;
MTHETA = 0.324104E-03;
XTHETA = -31.2141 ;
NB = 1.80138 ;
LB = -15.6431 ;
YB = -0.125678 ;
NP = -0.479147E-01;
LP = -1.46912 ;
YP = 0.248441 ;
NR = -0.349715 ;
LR = 0.198914 ;
YR = -0.995187 ;
NDR = -0.886573 ;
LDR = 1.68185 ;
YDR = 0.246049E-01;
NDA = -0.792129E-01;
LDA = -9.57478 ;
YDA = 0.160166E-02;
NDDT = -0.701138 ;
LDDT = -6.43482 ;
YDDT = 0.178196E-01;
YPHI = 0.120535 ;
PHIR = 0.253312 ;
%//
%//
%// *** Load A matrix:
%//
%// THETA = pitch angle (deg)
%// U = body axial velocity (ft/sec)
%// A = angle of attack (deg)
%// Q = body axis pitch rate (deg/sec)
%// PHI = Euler roll angle (deg)
%// B = sideslip angle (deg)
%// P = body axis roll rate (deg/sec)
%// R = body axis yaw rate (d/sec)
%//
A_VISTA = [ 0 0 0 1 0 0 0 0;
            XTHETA XU XA XQ 0 0 0 0;
            ZTHETA ZU ZA ZQ 0 0 0 0;
            MTHETA MU MA MQ 0 0 0 0;
            0 0 0 0 0 0 1 PHIR;
            0 0 0 0 YPHI YB YP YR;
            0 0 0 0 0 LB LP LR;
            0 0 0 0 0 NB NP NR];

```

```

%//
%//
%// *** Load B matrix:
%//
%// DE = elevator deflection (degrees)
%// DDT = differential elevator deflection (degrees)
%// DF = flap deflection (degrees)
%// DA = aileron deflection (degrees)
%// DR = rudder deflection (degrees)
%//
B_VISTA = [ 0 0 0 0 0;
            XDE 0 XDF 0 0;
            ZDE 0 ZDF 0 0;
            MDE 0 MDF 0 0;
            0 0 0 0 0;
            0 YDDT 0 YDA YDR;
            0 LDDT 0 LDA LDR;
            0 NDDT 0 NDA NDR];

```

Low Order Equivalent System Matlab® M-File

```

% Case1.m Holds information for case study one. F-16 flt cond
% M=.24 Alt = 1000 ft.
%

```

% BASIC AIRFRAME

```

thetan =[ 0          0 -2.6231e+000 -1.6349e+000 -3.4378e-002];
% 1/T1= -.021789 1/Ttheta2= -.60148

den =[ 1.0000e+000 1.1916e+000 -7.7178e-001 -8.4954e-002 -5.3371e-002];

% longitudinal denominator short period .59574 unstable
% -1.6421
% phugoid wp=.23357
% zeta=.31081

alphan =[ 0 -8.6103e-002 -2.6731e+000 3.8749e-003 -2.8108e-002];
% roots = -31.047 , w=.1025 zeta=.0087194

Nzn =[0 -4.4395e-001 -3.0682e-001 -1.3195e+001 -5.0418e-002 0];
% roots = 0, -.0038215, w=5.4514 zeta=.063037

% F-16 theta/Fs with FCS
Thetafsnm =[ 5.5246e+006 4.3949e+008 5.4568e+009 1.8883e+010 9.4786e+009];

```

```
Thetafsdm =[ 1.0000e+000 5.1040e+002 8.0361e+004 5.6223e+006 2.0384e+008  
2.6563e+009...  
1.6266e+010 6.5019e+010 1.9812e+011 2.5732e+011 8.5459e+008];
```

```
% zeros =  
%  
% -6.5200e+001  
% -8.7500e+000  
% -5.0000e+000  
% -6.0148e-001  
%  
% poles =  
%  
% -2.9500e+002  
% -1.1200e+002  
% -4.2809e+001+ 4.1990e+001i w=59.964  
% -4.2809e+001- 4.1990e+001i zeta= .7139  
% -8.3000e+000  
% -6.1634e+000  
% -4.1834e-001+ 4.1045e+000i w=4.1258  
% -4.1834e-001- 4.1045e+000i zeta= .1014  
% -2.4809e+000  
% -3.3296e-003  
%  
% k =  
% 5.5246e+006
```

```
% Short Period Approximation of Theta/Fs with FCS Jmin=.8 for match
```

```
nl =[ 2.9137e+000 1.7525e+000];  
% Ttheta2= -.60148
```

```
dl =[1.0000e+000 3.6427e+000 1.9503e+001 4.7696e+001 0];  
% roots = 0, -2.7865, w=4.1373 zeta=.10347
```

```
tl = 1.7129e-002;  
% time delay
```


Case Two

VISTA F-16 Aero Model Matlab® M-File

plant0160.m

%//

%// File: m1_6nat.mod

%// Created: 4-May-93 18:26:39

%//

%// Function:

%// This is a MATRIXx macro file which generates a linear
%// model in state space form of the F-16 VISTA. The file was
%// generated by the SRF VISTA simulation.

%//

%// Note: Set the MXFILE input parameter from TAE when running
%// VISTA, to generate this file.

%//

%//

%// *** Flight Condition:

%//

%// MACH = 0.6000000E+00 ALTITUDE = 0.1000000E+04 LOAD FACTOR =
1.0

%// VELOCITY (ft/sec) = 0.6673881E+03

%// Wings empty (gear up)

%// VISTA w/AIM-9Ls

%//

MACH = 0.6000000E+00;

ALTITUDE = 0.1000000E+04;

U = 0.6673881E+03;

%//

%// *** Mass Properties:

%//

%// WEIGHT = 0.2489260E+00 VPDOT = 0.7314248E-02 THRUST =
0.3697091E+04

%// IXX = 0.9466000E+04 IYY = 0.5902100E+05 IZZ = 0.6606500E+05

%// IXZ = 0.3850000E+03 X CG = 0.3747000E+02 Z CG = 0.9400000E+02

%// MAC = 0.1132000E+02 AREA = 0.3000000E+03 SPAN =
0.3000000E+02

%//

%//

%// *** Trim Solution:

%//

%// ALPHA = 0.2141754E+01 ELEV = -0.1833963E+01 TEF =

%// LEF = 0.1524682E+01 QBAR = 0.5142514E+03 CLQ = 0.1605574E+00

%// CMS = -0.4121684E-02 CDQ = 0.2391077E-01

%//

ALPHA = 0.2141754E+01;

ELEV = -0.1833963E+01;

QBAR = 0.5142514E+03;

CLA = 7.3578E-02;

%//

%// *** Longitudinal non-dimensional aero derivatives - stability axis:

%// positional units = 1/degrees, rate units = 1/radians

%//

%//	Cm	CL	CD
%// ALPHA (DEG)	1.6504E-03	7.3578E-02	6.2184E-04
%// ELEVATOR (DEG)	-1.1103E-02	1.2174E-02	-8.8401E-04
%// T.E. FLAP (DEG)	1.1290E-04	6.6787E-03	6.3172E-04
%// Q (RAD)	-5.4312E+00	2.9486E+00	1.0708E-01
%// ALPHA DOT (RAD)	-8.0615E-01	-1.0160E+00	0.0000E+00
%// U (VEL-FT/S)	-1.6021E-05	-1.7583E-05	4.5542E-06

%//

%// *** Lateral-directional non-dimensional aero derivatives:

%// positional units = 1/degrees, rate units = 1/radians

%//

%//	Cn	Cl	CY
%// BETA (DEG)	3.3487E-03	-1.3406E-03	-1.8871E-02
%// P (RAD)	-1.6441E-02	-4.2557E-01	7.1969E-02
%// R (RAD)	-4.9566E-01	-4.3089E-03	5.4002E-01
%// RUDDER (DEG)	-1.3291E-03	4.1147E-04	2.9031E-03
%// FLAPERON (DEG)	-1.3125E-04	-1.9704E-03	5.8733E-04
%// DIFF TAIL (DEG)	-1.0337E-03	-1.4890E-03	2.4404E-03

%//

%// *** Load coefficients:

%//

ZA = -1.26819 ;

MA = 3.04332 ;

XA = 56.2269 ;

ZDE = -0.207866 ;

MDE = -18.7807 ;

XDE = 15.3032 ;

ZDF = -0.114749 ;

MDF = 0.214610 ;

XDF = -4.36418 ;

ZQ = 0.992528 ;

MQ = -1.56356 ;

XQ = -24.7609 ;

ZU = -0.736040E-04;

MU = -0.507737E-03;

```

XU = -0.138611E-01;
ZTHETA = -.180311E-02;
MTHETA = 0.364510E-03;
XTHETA = -32.1775 ;
NB = 12.9947 ;
LB = -40.5076 ;
YB = -0.323310 ;
NP = -0.489432E-01;
LP = -4.67125 ;
YP = 0.377284E-01;
NR = -0.781803 ;
LR = -0.500673E-01;
YR = -0.996355 ;
NDR = -5.19528 ;
LDR = 12.6990 ;
YDR = 0.497382E-01;
NDA = -1.14296 ;
LDA = -55.0688 ;
YDA = 0.100626E-01;
NDDT = -4.60729 ;
LDDT = -40.7879 ;
YDDT = 0.418114E-01;
YPHI = 0.482141E-01;
PHIR = 0.373981E-01;
%//
%//
%// *** Load A matrix:
%//
%// THETA = pitch angle (deg)
%// U = body axial velocity (ft/sec)
%// A = angle of attack (deg)
%// Q = body axis pitch rate (deg/sec)
%// PHI = Euler roll angle (deg)
%// B = sideslip angle (deg)
%// P = body axis roll rate (deg/sec)
%// R = body axis yaw rate (d/sec)
%//
A_VISTA = [ 0 0 0 1 0 0 0 0;
            XTHETA XU XA XQ 0 0 0 0;
            ZTHETA ZU ZA ZQ 0 0 0 0;
            MTHETA MU MA MQ 0 0 0 0;
            0 0 0 0 0 0 1 PHIR;
            0 0 0 0 YPHI YB YP YR;
            0 0 0 0 0 LB LP LR;
            0 0 0 0 0 NB NP NR];

```

```

%//
%//
%// *** Load B matrix:
%//
%// DE = elevator deflection (degrees)
%// DDT = differential elevator deflection (degrees)
%// DF = flap deflection (degrees)
%// DA = aileron deflection (degrees)
%// DR = rudder deflection (degrees)
%//
B_VISTA = [ 0 0 0 0 0;
            XDE 0 XDF 0 0;
            ZDE 0 ZDF 0 0;
            MDE 0 MDF 0 0;
            0 0 0 0 0;
            0 YDDT 0 YDA YDR;
            0 LDDT 0 LDA LDR;
            0 NDDT 0 NDA NDR];

```

Low Order Equivalent System Matlab® M-File

```

% CASE2.M Holds information for case study one. F-16 flt cond
% M=.24 Alt = 1000 ft.
%

```

% BASIC AIRFRAME

```

thetan =[ 0 0 -18.7807 -24.7182 -0.4240];
% 1/T1=-.0174 1/Ttheta2=-1.2988

den =[ 1.0000 2.8456 -1.0072 -0.0124 -0.0279];

% longitudinal denominator short period .3816 unstable
% -3.1636
% phugoid w=.1521
% zeta=.209

alphan =[ 0 -0.2079 -18.9694 -0.2700 -0.0406];
% roots = -91.2436, w= .0463 zeta= .1536

Nzn =[ 0 -3.8281 -6.7978 -506.9045 -7.9460 0];
% roots = 0, -.0157, w=11.5061 zeta= .0765

```

% F-16 theta/Fs with FCS

Thetafsnm =[3.9554e+007 2.9764e+009 2.6365e+010 2.9307e+010];

Thetafsdm =[1.0000e+000 5.0700e+002 9.6002e+004 1.2671e+007 8.6437e+008
1.1731e+010...
1.3789e+011 1.0165e+012 2.0168e+012 3.1365e+010];

% Theta/Fs with FCS

% zeros =

%

% -6.5200e+001

% -8.7500e+000

% -1.2988e+000

%

% poles =

%

% -2.9500e+002

% -4.3042e+001+ 1.3796e+002i

% -4.3042e+001- 1.3796e+002i

% -1.1200e+002

% -1.3640e+000+ 1.0934e+001i

% -1.3640e+000- 1.0934e+001i

% -8.3000e+000

% -2.8772e+000

% -1.5675e-002

%

% k = 3.9554e+007

%

% Short Period Approximation of Theta/Fs with FCS Jmin=3.7 for match

nl =[4.0315e+000 5.2361e+000];

% 1/Ttheta2= -1.299

dl =[1.0000e+000 5.7607e+000 1.3135e+002 3.6006e+002 0];

% roots 0, -2.926, w=11.09 zeta=.128

tl = 4.7620e-003;

% time delay

Appendix C

Low Order Equivalent System Matching Matlab® M-Files

```

function[numlos,denlos,taulos]=match(numhos,denhos,tauhos,mode)
%
% MATCH.M
%
% [Numlos,Denlos,Taulos]=MATCH(Numhos,Denhos,Taulos)
%
% Where:
%
% Numhos = Numerator of High-Order System
% Denhos = Denominator of High-Order System
% Tauhos = Delay of High-Order System
% Numlos = Numerator of Low-Order System Match
% Denlos = Denominator of Low-Order System Match
% Taulos = Equiv. Delay of Low-Order System Match
%
% The user selects the transfer function form to match --
%
% Pilot Crossover      K*(s+1/Tl)
% Model                ----- *exp(-s*tau)
%                    (s+1/Ti)
%
% Pitch Model          K*(s+1/Tt1)*(s+1/Tt2)
%                    -----*exp(-s*tau)
%                    (s^2+2*Zp*Wp+Wp^2)*(s^2+2*Zsp*Wsp*s+Wsp^2)
%
% Short Period         K*(s+1/Tt2)
% Pitch Model          -----*exp(-s*tau)
%                    s*(s^2+2*Zsp*Wsp*s+Wsp^2)
%
% Roll Model           K*(s^2+2*Zr*Wr*Wr^2)*exp(-s*tau)
%                    -----
%                    (s+1/Ts)*(s+1/Tr)*(s^2+2*Zd*Wd*s+Wd^2)
%
% This file runs a simplex search routine to match the
% desired form so that the following performance index
% is minimized between .1 and 10 rad/s.
%
% J = (20/N)* sum(n)[(gainhos-gainlos)^2+.02*(phzhos-phzlos)^2]
%
% The magnitudes and phases of the high and low order systems
% are plotted along with the appropriate mis-match envelopes.
%
% See MIL-STD-1797A, pp. 181, 681-685.

```

```

%
% C. Edkins -- 15 Oct. 92           Revised 14 Jan. 93
%
if(nargin>4),error('Incorrect Number of Input Arguments'),end
if(nargin<3),error('Incorrect Number of Input Arguments'),end
XO=0;
%
%%%%%%%%%%%%%%%%%%%%%%%%%%%%%%%%%%%%%%%%%%%%%%%%%%%%%%%%%%%%%%%%%%%%%%%%
%
% Compute High-Order Mag & Phase -- Input Model Form           %
%%%%%%%%%%%%%%%%%%%%%%%%%%%%%%%%%%%%%%%%%%%%%%%%%%%%%%%%%%%%%%%%%%%%%%%%
%
w=logspace(-1,1,40);
[maghos,phzhos,w]=bode(numhos,denhos,w);
dbmaghos=20*log10(maghos);
phzhos=phzhos-tauhos*w*180/pi;
if nargin==3
mode=menu('Select Type of Match','Pilot','Pitch','Short-Period Pitch','Roll');
disp(''),end
%
%
%%%%%%%%%%%%%%%%%%%%%%%%%%%%%%%%%%%%%%%%%%%%%%%%%%%%%%%%%%%%%%%%%%%%%%%%
%
% Pilot Model Match                                           %
%%%%%%%%%%%%%%%%%%%%%%%%%%%%%%%%%%%%%%%%%%%%%%%%%%%%%%%%%%%%%%%%%%%%%%%%
%
if mode==1
X=[5,2,5,.1];
xmin=fmins('pmatch',X,[],[],w,dbmaghos,phzhos);
jmin=pmatch(xmin,w,dbmaghos,phzhos)
x=xmin;
disp(''),disp(['In Transfer Function Form: K*(s+a)*exp(-st)/(s+b): '])
disp(['K = ',num2str(x(1))])
disp(['a = ',num2str(x(2))])
disp(['b = ',num2str(x(3))])
disp(['t = ',num2str(x(4))])
numlos=x(1)*[1,x(2)];
denlos=[1,x(3)];
taulos=x(4);

```



```

end
%
%%%%%%%%%%%%%%%%%%%%%%%%%%%%%%%%%%%%%%%%%%%%%%%%%%%%%%%%%%%%%%%%%%%%%%%%
%
%
%
%           Short Period Pitch Match           %
%%%%%%%%%%%%%%%%%%%%%%%%%%%%%%%%%%%%%%%%%%%%%%%%%%%%%%%%%%%%%%%%%%%%%%%%
%
%
%
%
if mode==3
    disp(['Note: 1/T-theta-2 is the Largest Zero in the Pure Pitch EOM'])
    tt2=input('Input Actual 1/T-Theta-2 -- Fixed Value ');disp("")
    X=[15,4,5,1];
    xmin=fmins('tspmatch',X,[],[],w,dbmaghos,phzhos,tt2);
    jmin=tspmatch(xmin,w,dbmaghos,phzhos,tt2)
    x=xmin;
    b=2*x(2)*x(3);
    c=x(3)^2;
    disp(['In Transfer Function Form: K(s+a)exp(-st)/s(s^2+bs+c): '])
    disp(['K = ',num2str(x(1))])
    disp(['a = ',num2str(tt2)])
    disp(['b = ',num2str(b),'      Zeta-sp = ',num2str(x(2))])
    disp(['c = ',num2str(c),'      W-sp = ',num2str(x(3))])
    disp(['t = ',num2str(x(4))])
    numlos=x(1)*[1,tt2];
    denlos=conv([1,0],[1,b,c]);
    taulos=x(4);
end
%
%%%%%%%%%%%%%%%%%%%%%%%%%%%%%%%%%%%%%%%%%%%%%%%%%%%%%%%%%%%%%%%%%%%%%%%%
%
%
%
%           Draw Bode Comparison Plots           %
%%%%%%%%%%%%%%%%%%%%%%%%%%%%%%%%%%%%%%%%%%%%%%%%%%%%%%%%%%%%%%%%%%%%%%%%
%
%
%
%
matchplt(numhos,denhos,tauhos,numlos,denlos,taulos)
return

```

```

function J=tspmatch(x,w,dbmaghos,phzhos,tt2);
%
% TSPMATCH.M
% This file works with MATCH.M to find the
% best low-order equivalent system match
% to the short-period pitch model.
%
% C.Edkins -- 15 Oct. 92
%
wlm=length(w);
num1=x(1)*[1,tt2];
den1=conv([1,0],[1,2*x(2)*x(3),x(3)^2]);
[maglos,phzlos]=bode(num1,den1,w);
dbmaglos=20*log10(maglos);
phzlos=phzlos-x(4)*w'*180/pi;
mdif=dbmaghos-dbmaglos;
pdif=phzhos-phzlos;
J=20/wlm*(mdif*mdif+.02*pdif*pdif);
return

```

```

function []=matchplt(numhos,denhos,tauhos,numlos,denlos,taulos)
%
% MATCHPLT(Numhos,Denhos,Tauhos,Numlos,Denlos,Taulos)
%
% This file makes magnitude and phase plots of a
% high-order system and its low-order equivalent so that
% the user can determine the accuracy of the match. This
% file also plots the maximum diference boundries, given
% in MIL-STD-1797, p. 181.
%
% This file is called by the MATCH.M file, but can be run
% separately.
%
% Where:
%
% Numhos = Numerator of High-Order System
% Denhos = Denominator of High-Order System
% Tauhos = Delay of High-Order System
% Numlos = Numerator of Low-Order System
% Denlos = Denominator of Low-Order System
% Taulos = Equiv. Delay of Low-Order System
%
% C. Edkins -- 15 Oct. 92

```

```

%
if(nargin~=6),error('Incorrect Number of Input Arguments'),end
%
%%%%%%%%%%
%%%%%%%%%
%
%%%%%%%%%
%       Find Magnitudes and Phases           %
%%%%%%%%%
%%%%%%%%%
%
w=logspace(-1,1,200);
[maglos,phzlos,w]=bode(numlos,denlos,w);
dbmaglos=20*log10(maglos);
phzlos=phzlos-taulos*w'*180/pi;
[maghos,phzhos,w]=bode(numhos,denhos,w);
dbmaghos=20*log10(maghos);
phzhos=phzhos-tauhos*w'*180/pi;
%
%
%%%%%%%%%
%%%%%%%%%
%       Find Differences and Envelopes      %
%%%%%%%%%
%%%%%%%%%
%
magdif=dbmaghos-dbmaglos;
phzdif=phzhos-phzlos;
magnumu=[3.16,31.61,22.79];
magdenu=[1,27.14,1.84];
magnuml=[.095,9.92,2.15];
magdenl=[1,11.6,4.95];
phznumu=[68.89,1100.12,-275.22];
phzdenu=[1,39.94,9.99];
phznuml=[475.32,184100,29460];
phzdenl=[1,11.66,.039];
[magu,p]=bode(magnumu,magdenu,w);
[magl,p]=bode(magnuml,magdenl,w);
[m,phzu]=bode(phznumu,phzdenu,w);
[m,phzl]=bode(phznuml,phzdenl,w);
magu=20*log10(magu);
magl=20*log10(magl);
phzu=phzu+.006*w'*180/pi;

```

```

phzl=phzl-.0072*w*180/pi;
%
%
%%%%%%%%%
%%%%%%%%%
%
%           Draw Plots           %
%%%%%%%%%
%%%%%%%%%
%
%
hold off
axis([-1,1,-40,40]);
semilogx(w,dbmaghos)
xlabel('Frequency (rad/sec)')
ylabel('Mag. (dB)')
hold on
grid
semilogx(w,dbmaglos,'--')
title('Bode Magnitude Plot of High ( ) and Low-Order (--) System')
pr=menu('Do You Want a Hard Copy of This Plot?','Yes','No');
if (pr==1),print,end
%
hold off
axis([-1,1,-360,180]);
semilogx(w,phzhos)
xlabel('Frequency (rad/sec)')
ylabel('Phase (Deg.)')
hold on
grid
semilogx(w,phzlos,'--')
title('Bode Phase Plot of High ( ) and Low-Order (--) System')
pr=menu('Do You Want a Hard Copy of This Plot?','Yes','No');
if (pr==1),print,end
%
hold off
axis([-1,1,-20,20]);
semilogx(w,magu)
xlabel('Frequency (rad/sec)')
ylabel('Mag. (dB)')
title('Bode Magnitude Difference with Envelope')
hold on
grid
semilogx(w,magl)
semilogx(w,magdif)

```

```
pr=menu('Do You Want a Hard Copy of This Plot?','Yes','No');
if (pr==1),print,end
%
hold off
axis([-1,1,-180,180]);
semilogx(w,phzu)
xlabel('Frequency (rad/sec)')
ylabel('Phase (Deg.)')
title('Bode Phase Difference with Envelope')
hold on
grid
semilogx(w,phzl)
semilogx(w,phzdif)
pr=menu('Do You Want a Hard Copy of This Plot?','Yes','No');
if (pr==1),print,end
hold off
return
```

Appendix D
Pilot Transfer Functions

Case One (Optimal Control Model Pilot) Matlab® M-Files

```
% Case1.m Holds information for case study one. F-16 flt cond
% M=.24 Alt = 1000 ft.
%

% Pilot transfer functions (OCM)

% for Theta/Fs or Qickening=1.66

%% Pilot Numerator
yp166n =[9.0788e+002 -2.3256e+004 1.8481e+005 3.4891e+005 6.5495e+006
2.4703e+007....
6.7698e+007 2.1525e+008 1.6489e+008 4.7852e+006];

%% Pilot Denominator
yp166d =[1.0000e+000 4.8998e+001 1.0866e+003 1.3883e+004 1.1745e+005
8.4124e+005....
2.5732e+006 1.0237e+007 9.9357e+006 4.0024e+006 7.2773e+005];

%% Pilot transfer function for Gamma/Fs no Quickening

%% Pilot Numerator
ypn =[4.2698e+003 -1.1154e+005 8.6775e+005 2.7193e+006 1.7514e+007
7.1624e+007....
5.1180e+007 5.3459e+006];

%% Pilot Denominator
ypd =[1.0000e+000 4.7641e+001 1.0028e+003 1.1597e+004 8.9649e+004
4.6178e+005....
1.9147e+006 1.0105e+006 2.6680e+005];

%% Pilot transfer function for Quickening = 0.20

%% Pilot Numerator
yp2n =[1.5224e+003 -2.5087e+004 -1.5766e+004 2.6343e+006 2.2569e+007
1.5233e+008...
7.2845e+008 2.3111e+009 6.2931e+009 1.1360e+010 6.9905e+009
3.3951e+008];

%% Pilot Denominator
yp2d =[1.0000e+000 5.8107e+001 1.5532e+003 2.4785e+004 2.6083e+005
2.1947e+006...
1.1272e+007 4.4009e+007 1.3034e+008 2.0677e+008 2.6606e+008 1.1848e+008
2.7142e+007];
```

%% Pilot transfer function for Quickening = 0.60

%% Pilot Numerator

yp6n=[1.1062e+003 -2.7627e+004 1.8609e+005 1.1124e+006 4.1851e+006
1.8704e+007...
3.5096e+007 1.9659e+007 7.4324e+005];

%% Pilot Denominator

yp6d=[1.0000e+000 5.0096e+001 1.1232e+003 1.4219e+004 1.1184e+005
7.4089e+005...
1.1670e+006 1.1068e+006 4.4225e+005 9.0339e+004];

%% Pilot transfer function for Quickening = 1.00

%% Pilot Numerator

yp10n =[9.7168e+002 -2.4841e+004 1.7935e+005 8.3819e+005 3.4473e+006
1.5253e+007...
2.2637e+007 1.0406e+007 3.3534e+005];

%% Pilot Denominator

yp10d =[1.0000e+000 4.9240e+001 1.0813e+003 1.3311e+004 1.0221e+005
6.5640e+005...
1.0022e+006 7.6168e+005 2.7297e+005 4.7873e+004];

%% Pilot transfer function for Quickening = 1.80

%% Pilot Numerator

yp18n =[9.0634e+002 -2.3474e+004 1.7583e+005 7.0420e+005 3.1398e+006
1.3676e+007...
1.6366e+007 5.6329e+006 1.5322e+005];

%% Pilot Denominator

yp18d =[1.0000e+000 4.8729e+001 1.0567e+003 1.2790e+004 9.6743e+004
6.1053e+005...
9.1299e+005 5.7418e+005 1.8096e+005 2.4783e+004];

%% Pilot transfer function for Quickening = 2.00

%% Pilot Numerator

yp20n =[9.0402e+002 -1.9842e+004 8.2818e+004 1.3967e+006 5.8883e+006
2.6011e+007...
6.9789e+007 6.7780e+007 2.0474e+007 5.4009e+005];


```

%% Pilot Denominator
yp20d = [ 1.0000e+000 5.2812e+001 1.2558e+003 1.7107e+004 1.4897e+005
1.0049e+006...
3.4106e+006 4.2900e+006 2.4571e+006 7.2688e+005 9.1463e+004];

```

Case Two (Neal-Smith Pilot) Matlab® M-Files

```

% CASE2.M Holds information for case study one. F-16 fit cond
% M=.24 Alt = 1000 ft.
%

```

```

% Pilot transfer functions (Neal-Smith)

```

```

% Theta/Fs or Quickening = 0.77

```

```

yp77n = [ -13.6711 86.5837 182.2814];

```

$$Y_p = \frac{184(0.6s+1)e^{-.25s}}{(2.1s+1)}$$

```

yp77d = [ 0.2605 2.2078 0.9923];

```

```

%% Pilot transfer function for Quickening = 0.15

```

```

yp15n = [ -4.9780e+001 3.1527e+002 6.6373e+002];

```

$$Y_p = \frac{669(0.6s+1)e^{-.25s}}{(2.1s+1)}$$

```

yp15d = [ 2.6047e-001 2.2078e+000 9.9228e-001];

```

```

%% Pilot transfer function for Quickening = 0.28

```

```

yp28n = [ -29.1432 184.5736 388.5760];

```

$$Y_p = \frac{392(0.6s+1)e^{-.25s}}{(2.6s+1)}$$

```

yp28d = [ 0.3225 2.7040 0.9923];

```

```

%% Pilot transfer function for Quickening = 0.50

```

```

yp5n = [ -19.1187 121.0852 254.9162];

```

$$Y_p = \frac{257(0.6s+1)e^{-.25s}}{(2.6s+1)}$$

```

yp5d = [ 0.3225 2.7040 0.9923];

```

%%%% Pilot transfer function for Quickening = 1.00

yp10n = [-17.2805 109.4433 230.4069];

$$Y_p = \frac{232(0.6s+1)e^{-.25s}}{(2.6s+1)}$$

yp10d = [0.3225 2.7040 0.9923];

%%%% Pilot transfer function for Quickening = 1.40

yp14n = [-17.2210 109.0662 229.6131];

$$Y_p = \frac{231(0.6s+1)e^{-.25s}}{(2.6s+1)}$$

yp14d = [0.3225 2.7040 0.9923];

%%%% Basic Gamma/Fs no Quickening

ypn = [-14.4075 110.6124 37.1807];

$$Y_p = \frac{37.5(3.1s+1)e^{-.25s}}{(0.6s+1)}$$

ypd = [0.0744 0.7194 0.9923];

Appendix E

Case Study Root Mean Square Results

Table E.1
Case One Root Mean Square (RMS) Results
Mach number = 0.24 Pressure Altitude = 1,000 feet

Quickening Time Constant	Flight Path Error RMS (deg)	Input Rate RMS (lb/sec)
0 - Nonquickened	0.747	30.54
0.20	0.744	51.79
0.60	0.683	47.79
1.00	0.681	45.03
1.66 - Theoretically Determined	0.652	43.79
1.80 - Simulator Determined	0.659	43.69
2.00	0.672	43.38

Table E.2
Case Two Root Mean Square (RMS) Results
Mach number = 0.60 Pressure Altitude = 1,000 feet

Quickening Time Constant	Flight Path Error RMS (deg)	Input Rate RMS (lb/sec)
0 - Nonquickened	1.307	102.6
0.15	0.423	unstable
0.28 - Simulator Determined	0.759	139.1
0.50	0.951	117.5
0.77 - Theoretically Determined	0.938	111.9
1.00	0.814	122.0
1.40	0.732	128.2

Case Study Root Mean Square (RMS) Calculation Matlab® M-Files

```

% ver2 - Calculates RMS values for quickened system
%     K - Quickening Gain
%     tau - Quickening Time Constant
%     pilotn - pilot transfer function numerator
%     pilotd - pilot transfer function denominator
%     nac - Aircraft Pitch Attitude to Stick Force numerator
%     dac - Aircraft Pitch Attitude to Stick Force denominator
%     T - Aircraft 1/ Tθ2
%     Yg - Flight Path Error RMS
%     Yu - Input Rate RMS
%     J - Flight Path Error RMS + Input Rate RMS
%     nc - Flight Path to Flight Path Command transfer function numerator
%     dc - Flight Path to Flight Path Command transfer function denominator

function [Yg,Yu,J,nc,dc]=ver2(K,tau,pilotn,pilotd,nac,dac,T)

% Set up quickening transfer function and flight path to pitch angle transfer function
Tn=T;Td=[1 T];
nQ=K*[1 0];dQ=[1 1/tau];
Dn1=conv(dQ,Tn);
Dn2=conv(nQ,Td);
[Dn1,Dn2]=addcon(Dn1,Dn2);
Dn=Dn1+Dn2;
Dd=conv(dQ,Tn);

% Calculates flight path error rms
[nc,dc]=cloop(conv(Dn,conv(pilotn,conv(nac,Tn))),conv(Dd,conv(pilotd,conv(dac,Td))))
fn=2*Tn;
fd=conv(Td,[1 .5 .25]);
[a,b,c,d]=tf2ss(conv(fn,dc-nc),conv(fd,dc));
disp('gamma error minreal')
Yg=sqrt(c*lyap(a,b*b')*c');

% Calculates input rate rms
nu=conv(dac,conv(Td,conv(pilotn,Dn)));
du1=conv(pilotd,conv(Dd,conv(dac,Td)));
du2=conv(nac,conv(Tn,conv(pilotn,Dn)));
[du1,du2]=addcon(du1,du2);
du=du1+du2;
disp('u minreal')
[Gn,Gd]=minreal(conv([1 0],conv(fn,nu)),conv(fd,du));
[A,B,C,D]=tf2ss(Gn,Gd);

```

```
[A,B,C,D]=canon(A,B,C,D,'modal');
Yu=sqrt((C*lyap(A,B*B')*C'));
```

```
J=Yg+Yu;
```

```
% Workbas.m - Calculates RMS of nonquickened system
% pilotn - pilot transfer function numerator
% pilotd - pilot transfer function denominator
% nac - Aircraft Pitch Attitude to Stick Force numerator
% dac - Aircraft Pitch Attitude to Stick Force denominator
% T - Aircraft 1/  $T_{\theta 2}$ 
% Ygb - Flight Path Error RMS
% Yub - Input Rate RMS
% Jb - Flight Path Error RMS + Input Rate RMS
```

```
function [Ygb,Yub,Jb]=workbas(pilotn,pilotd,nac,dac,T)
```

```
% Set up noise filter and close loop system
[ncg,dcg]=cloop(conv(pilotn,conv(nac,T)),conv(pilotd,conv(dac,[1 T])));
fn=2*T;
fd=conv([1 T],[1 .5 .25]);
```

```
% Calculates flight path error rms
[a,b,c,d]=tf2ss(conv(fn,dcg-ncg),conv(fd,dcg));
[a,b,c,d]=canon(a,b,c,d,'modal');
Ygb=sqrt(c*lyap(a,b*b')*c');
```

```
% Calculates input rate rms
nU1=conv(pilotn,conv([1 T],dac));
Ua=conv(pilotd,conv([1 T],dac));
Ub=conv(pilotn,conv(T,nac));
[Ua,Ub]=addcon(Ua,Ub);
dU1=Ua+Ub;
[aa,bb,cc,dd]=tf2ss(conv(fn,conv([1 0],nU1)),conv(fd,dU1));
[aa,bb,cc,dd]=canon(aa,bb,cc,dd,'modal');
Yub=sqrt(cc*lyap(aa,bb*bb')*cc');
```

```
Jb=Ygb+Yub;
```

Appendix F
Cooper-Harper Rating Criteria

TASK PERFORMANCE CRITERIA

ILS OFFSET TASK

Gross Acquisition

Adequate Criteria:

1 dot above/below within 5 seconds
1 overshoot

Desired Criteria:

1/2 dot within 5 seconds
1 overshoot

Fine Tracking

Adequate Criteria:

maintain within 1/2 dot with no overshoots
maintain airspeed within +10 to -5 knots indicated

Desired Criteria:

maintain within 1/4 dot with no overshoots
maintain airspeed within +/- 5 knots indicated

LOW ALTITUDE FLIGHT PATH TRACKING TASK

Adequate Criteria:

maintain target within 3.3 mil outside diameter FPM 50% of time

Desired Criteria:

maintain target within 3.3 mil outside diameter FPM 75% of time

AIM-OFF POINT TRACKING TASK

Adequate Criteria:

maintain target within 3.3 mil outside diameter FPM 50% of time

Desired Criteria:

maintain target within 3.3 mil outside diameter FPM 75% of time

Appendix G

LAHOS Aircraft Configurations and Pilot Transfer Functions for Root Mean Square Database

Table G.1
LAHOS CHR 1-3 Aircraft Configurations Used for Database

Configuration	Short Period Frequency, ω_{sp} (rad/sec)	Short Period Damping Ratio, ξ_{sp}	Control System	Pilot Reported CHR
2A	2.3	0.57	$\frac{0.4s+1}{.1s+1}$	2
2C	2.3	0.57	$\frac{0.2s+1}{.1s+1}$	1.5
2-1	2.3	0.57	None	2
2-2	2.3	0.57	$\frac{1}{.1s+1}$	2
4C	2.0	1.06	$\frac{0.2s+1}{.1s+1}$	2
4-1	2.0	1.06	None	2
4-7	2.0	1.06	$\frac{144}{s^2+16.8s+14}$	3
5-6	3.9	0.54	$\frac{256}{s^2+22.4s+256}$	3

Table G.2
Neal-Smith Pilot Models for LAHOS CHR 1-3

Configuration	Pilot Transfer Function γ (degrees) / F_s (lbs)
2A	$\frac{5.90(0.6s+1)e^{-.25s}}{1.1s+1}$
2C	$\frac{10.3(s+1)e^{-.25s}}{2s+1}$
2-1	$\frac{4.78(2.6s+1)e^{-.25s}}{2.1s+1}$
2-2	$\frac{7.91(1.5s+1)e^{-.25s}}{2.5s+1}$
4-C	$\frac{7.40(1.6s+1)e^{-.25s}}{1.1s+1}$
4-1	$\frac{4.278(2s+1)e^{-.25s}}{s+1}$
4-7	$\frac{5.88(0.6s+1)e^{-.25s}}{0.1s+1}$
5-6	$\frac{6.73(0.8s+1)e^{-.25s}}{0.1s+1}$

Table G.3
LAHOS CHR 4-6 Aircraft Configurations Used for Database

Configuration	Short Period Frequency, ω_{sp} (rad/sec)	Short Period Damping Ratio, ξ_{sp}	Control System	Pilot Reported CHR
1-1	1.0	0.74	None	4
1-3	1.0	0.74	$\frac{1}{0.25s+1}$	6
1-6	1.0	0.74	$\frac{256}{s^2+22.4s+256}$	5
2-6	2.3	0.57	$\frac{256}{s^2+22.4s+256}$	5
4-4	2.0	1.06	$\frac{1}{.5s+1}$	4
4-10	2.3	0.57	None	4
5-1	3.9	0.54	None	4

Table G.4
Neal-Smith Pilot Models for LAHOS CHR 4-6

Configuration	Pilot Transfer Function γ (degrees) / F_s (lbs)
1-1	$\frac{4.91(2.1s+1)e^{-25s}}{0.1s+1}$
1-3	$\frac{3.80(0.3s+1)e^{-25s}}{0.04s+1}$
1-6	$\frac{5.71(2.1s+1)e^{-25s}}{0.1s+1}$
2-6	$\frac{6.01(1.5s+1)e^{-25s}}{2s+1}$
4-4	$\frac{7.34(1.1s+1)e^{-25s}}{0.1s+1}$
4-10	$\frac{3.66(1.5s+1)e^{-25s}}{0.1s+1}$
5-1	$\frac{5.88(0.6s+1)e^{-25s}}{0.1s+1}$

Table G.5
LAHOS CHR 7-10 Aircraft Configurations Used for Database

Configuration	Short Period Frequency, ω_{sp} (rad/sec)	Short Period Damping Ratio, ξ_{sp}	Control System	Pilot Reported CHR
2-9	2.3	0.57	$\frac{36}{s^2+8.4s+36}$	10

Table G.6
Neal-Smith Pilot Models for LAHOS CHR 7-10

Configuration	Pilot Transfer Function γ (degrees) / F_s (lbs)
2-9	$\frac{6.47(0.1s+1)e^{-.25s}}{0.01s+1}$

Appendix H

Root Mean Square (RMS) Flight Test Handling Quality Regions

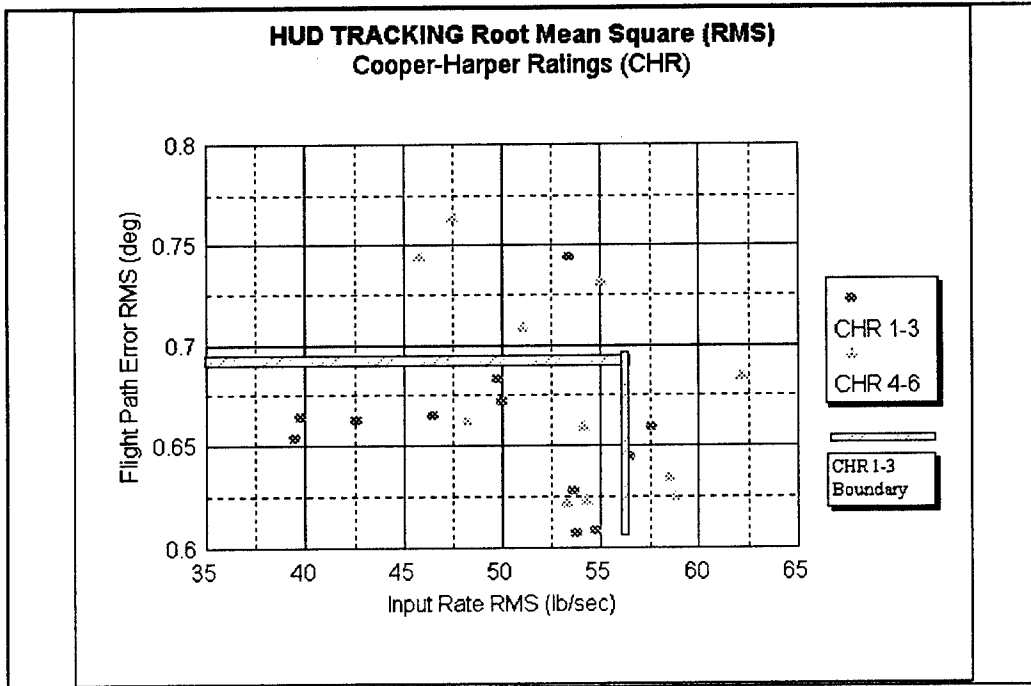


Figure H.1 HUD Tracking Flight Test RMS Handling Quality Regions

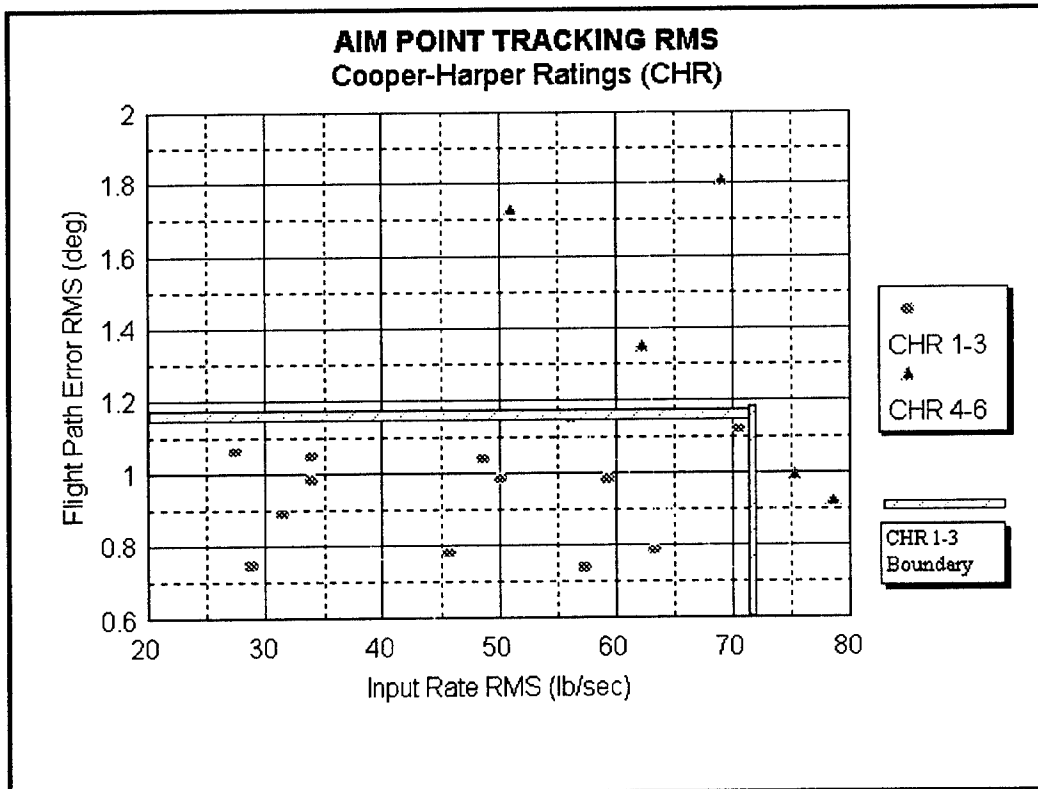


Figure H.2 Aim Point Tracking Flight Test RMS Handling Quality Regions

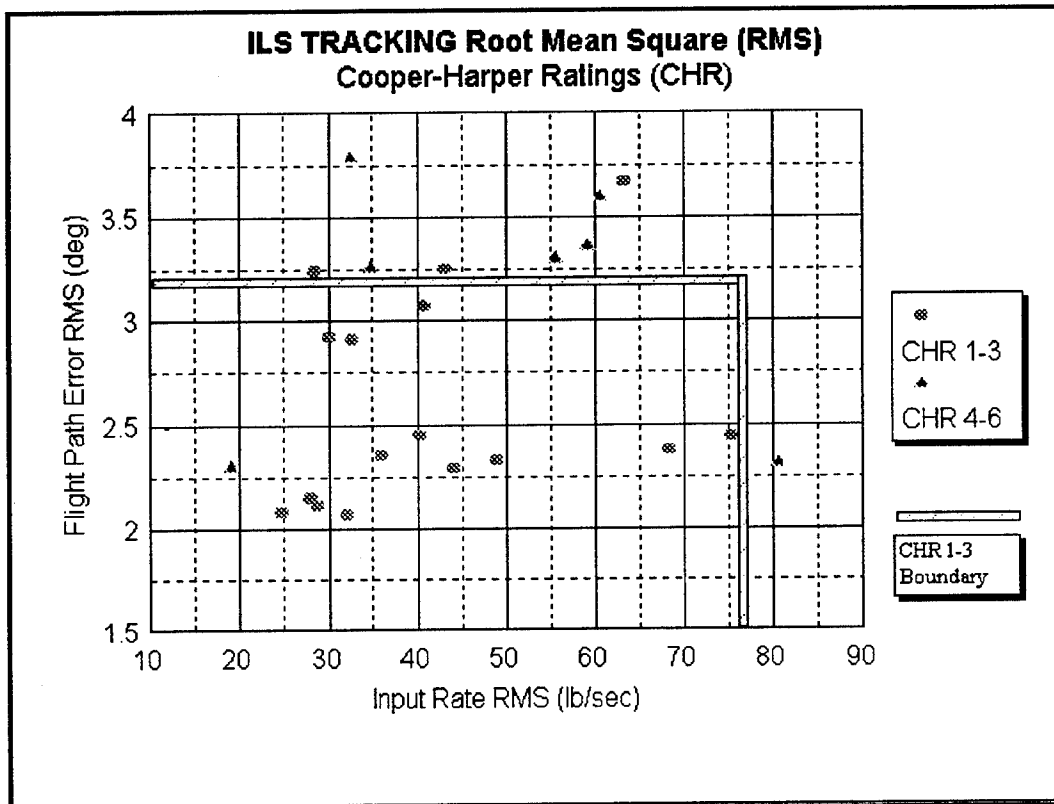


Figure H.3 ILS Tracking Flight Test RMS Handling Quality Regions

The data in Figures H.1 through H.3 were gathered from every attempt each pilot made during the flight test at the individual tasks with various quickening values. The RMS values and associated pilot reported Cooper-Harper ratings (CHRs) were then plotted for each task. Based on the limited data available, handling quality regions were determined. The resulting CHR 1-3 region was well defined for all the tasks, except the HUD tracking task. The Cooper-Harper Ratings were somewhat scattered compared to the RMS values in this task making the boundary very fuzzy. The region marked is the best estimate for the data obtained.

Bibliography

1. *Display Systems Dynamics Requirements for Flying Qualities*, AFWAL-TR-88-3017, Air Force Flight Dynamics Laboratory, Wright-Patterson AFB, OH, May 1988.
2. Edkins, Craig R., *The Prediction of Pilot Opinion Ratings Using Optimal and Sub-Optimal Pilot Models*, Air Force Institute of Technology, AFIT/ENY/GAE/94M-1, March 1994.
3. Franklin, Gene F., Powell, J. D., and Emami-Naeini, A., *Feedback Control of Dynamic Systems*, Addison-Wesley Publishing Company, New York: 1991.
4. Garg, Sanjay and David Schmidt, *Experimental Investigation Control/Display Augmentation Effects in a Compensatory Tracking Environment*, AIAA Atmospheric Flight Mechanics Conference, Minneapolis, Minnesota, August 1988.
5. Hall, J. R. and J. C. Penwill, *RAE Fast-Jet HUD Format-Specification Issue 2*, RAE FM WP(89)064, Military Simulation Section, Royal Aerospace Establishment, Bedford, England, September 1989.
6. Hawkins, Frank H., *Human Factors in Flight*, Gower Publishing Company, Vermont: 1987.
7. Huff, R. W. and G. K. Kessler, *Enhanced Displays, Flight Controls, and Guidance Systems for Approach and Landing*, Naval Air Test Center, Patuxent River, MD, 1990.
8. Knotts, L., Ball, J., Parrag, M., Lutz, T., *Test Pilot School Flight Syllabus and Background Material for the USAF NT-33A Variable Stability Aircraft*, September 1991.
9. Konnert, G. M., *A Limited Evaluation of the Optimum Head-Up Display Flight Path Marker Quickening Time Constant for Fighter Type Aircraft in the Low Altitude Arena*, AFFTC-TLR-94-83, Air Force Flight Test Center, Edwards AFB, CA, 1994.
10. Kwakernaak, Huibert and Raphael Sivan, *Linear Optimal Control Systems*, Wiley-Interscience, New York: 1972.
11. *Military Standard, Aircraft Display Symbolology*, MIL-STD-1787B, 1995.

12. *Military Standard, Flying Qualities of Piloted Vehicles*, MIL-STD-1797A, January 1990.
13. Sanjay, Gary and David K. Schmidt, *Optimal Cooperative Control Synthesis of Active Displays*, NASA CR 4058, 1987.
14. Thompson, P. M., *Minimum Flying Qualities, Vol. III: Program CC's Implementation of the Human Optimal Control Model*, WRDC-TR-89-3125, Air Force Flight Dynamics Laboratory, Wright-Patterson AFB, OH, January 1990 (AD-A218 562).
15. Turner, A. D. and Hattendorf, P. E., *Standardized Head-Up Display Symbology Evaluation*, AFFTC-TR-92-15, February 1993.

Vita

Captain Gary M. Konnert [REDACTED]. He attended the USAF Academy where he graduated in 1985 with a Bachelor of Science in Astronautical Engineering. After pilot training he was assigned to Wurtsmith AFB, Michigan from 1987 to 1992. Accumulating over 2,300 hours flying time in the Cessna T-37 and Boeing B-52G, he flew combat missions in the Persian Gulf. His duties as a B-52 training flight instructor pilot included training aircrew in both nuclear and conventional missions. He was highly experienced with Night Vision Goggles, low level, and air refueling. Entering the Air Force Institute of Technology (AFIT) in 1992 to study for a Masters of Science in Aeronautical Engineering, he was part of the joint AFIT/TPS program and was qualified in the Rockwell T-39. Following his study at AFIT he entered the USAF Test Pilot School (TPS) in 1994. After graduation he was assigned as a test pilot to the 420th Test Squadron, Edwards AFB, California working on the Northrup-Grumman B-2.

Permanent Address: [REDACTED]

REPORT DOCUMENTATION PAGE

Form Approved
OMB No. 0704-0188

Public reporting burden for this collection of information is estimated to average 1 hour per response, including the time for reviewing instructions, searching existing data sources, gathering and maintaining the data needed, and completing and reviewing the collection of information. Send comments regarding this burden estimate or any other aspect of this collection of information, including suggestions for reducing this burden, to Washington Headquarters Services, Directorate for Information Operations and Reports, 1215 Jefferson Davis Highway, Suite 1204, Arlington, VA 22202-4302, and to the Office of Management and Budget, Paperwork Reduction Project (0704-0188), Washington, DC 20503.

1. AGENCY USE ONLY (Leave blank)		2. REPORT DATE March 1995	3. REPORT TYPE AND DATES COVERED Master's Thesis	
4. TITLE AND SUBTITLE Analysis of Heads-Up Display Quickening Versus Handling Qualities			5. FUNDING NUMBERS	
6. AUTHOR(S) KONNERT, Gary M., Capt, USAF				
7. PERFORMING ORGANIZATION NAME(S) AND ADDRESS(ES) AFIT/ENY Dr Brad Liebst WPAFB OH 45433-7765			8. PERFORMING ORGANIZATION REPORT NUMBER AFIT/GAE/ENY/95M-01	
9. SPONSORING / MONITORING AGENCY NAME(S) AND ADDRESS(ES) USAF/TPS/TSD LTC Dan Gleason Edwards AFB, CA 93524-6485			10. SPONSORING / MONITORING AGENCY REPORT NUMBER	
11. SUPPLEMENTARY NOTES				
12a. DISTRIBUTION / AVAILABILITY STATEMENT Approved for public release; Distribution Unlimited			12b. DISTRIBUTION CODE	
13. ABSTRACT (Maximum 200 words) This study investigated an analytical means of selecting the quickening time constant for the standardized Heads-Up Display flight path marker. The theoretically determined time constant allowed a faster, less resource intensive means of selecting the quickening time constant. The theoretically best time constant for pilot-aircraft handling qualities was equal to the airframe pitch attitude high frequency zero time constant, T-theta-2. Flight test indicated an empirical, more labor intensive method yielded better handling qualities, even though paper analysis indicated the theoretical method was better. The theoretically determined time constant gave slightly lower handling qualities. but was less costly to implement than the empirical method.				
14. SUBJECT TERMS HUD, Heads-Up Display, Quickening, NT-33, F-16			15. NUMBER OF PAGES 131	
			16. PRICE CODE	
17. SECURITY CLASSIFICATION OF REPORT Unclassified	18. SECURITY CLASSIFICATION OF THIS PAGE Unclassified	19. SECURITY CLASSIFICATION OF ABSTRACT Unclassified	20. LIMITATION OF ABSTRACT UL	

GENERAL INSTRUCTIONS FOR COMPLETING SF 298

The Report Documentation Page (RDP) is used in announcing and cataloging reports. It is important that this information be consistent with the rest of the report, particularly the cover and title page. Instructions for filling in each block of the form follow. It is important to *stay within the lines* to meet *optical scanning requirements*.

Block 1. Agency Use Only (Leave blank).

Block 2. Report Date. Full publication date including day, month, and year, if available (e.g. 1 Jan 88). Must cite at least the year.

Block 3. Type of Report and Dates Covered. State whether report is interim, final, etc. If applicable, enter inclusive report dates (e.g. 10 Jun 87 - 30 Jun 88).

Block 4. Title and Subtitle. A title is taken from the part of the report that provides the most meaningful and complete information. When a report is prepared in more than one volume, repeat the primary title, add volume number, and include subtitle for the specific volume. On classified documents enter the title classification in parentheses.

Block 5. Funding Numbers. To include contract and grant numbers; may include program element number(s), project number(s), task number(s), and work unit number(s). Use the following labels:

C - Contract	PR - Project
G - Grant	TA - Task
PE - Program Element	WU - Work Unit Accession No.

Block 6. Author(s). Name(s) of person(s) responsible for writing the report, performing the research, or credited with the content of the report. If editor or compiler, this should follow the name(s).

Block 7. Performing Organization Name(s) and Address(es). Self-explanatory.

Block 8. Performing Organization Report Number. Enter the unique alphanumeric report number(s) assigned by the organization performing the report.

Block 9. Sponsoring/Monitoring Agency Name(s) and Address(es). Self-explanatory.

Block 10. Sponsoring/Monitoring Agency Report Number. (If known)

Block 11. Supplementary Notes. Enter information not included elsewhere such as: Prepared in cooperation with...; Trans. of...; To be published in.... When a report is revised, include a statement whether the new report supersedes or supplements the older report.

Block 12a. Distribution/Availability Statement. Denotes public availability or limitations. Cite any availability to the public. Enter additional limitations or special markings in all capitals (e.g. NOFORN, REL, ITAR).

DOD - See DoDD 5230.24, "Distribution Statements on Technical Documents."

DOE - See authorities.

NASA - See Handbook NHB 2200.2.

NTIS - Leave blank.

Block 12b. Distribution Code.

DOD - Leave blank.

DOE - Enter DOE distribution categories from the Standard Distribution for Unclassified Scientific and Technical Reports.

NASA - Leave blank.

NTIS - Leave blank.

Block 13. Abstract. Include a brief (*Maximum 200 words*) factual summary of the most significant information contained in the report.

Block 14. Subject Terms. Keywords or phrases identifying major subjects in the report.

Block 15. Number of Pages. Enter the total number of pages.

Block 16. Price Code. Enter appropriate price code (*NTIS only*).

Blocks 17. - 19. Security Classifications. Self-explanatory. Enter U.S. Security Classification in accordance with U.S. Security Regulations (i.e., UNCLASSIFIED). If form contains classified information, stamp classification on the top and bottom of the page.

Block 20. Limitation of Abstract. This block must be completed to assign a limitation to the abstract. Enter either UL (unlimited) or SAR (same as report). An entry in this block is necessary if the abstract is to be limited. If blank, the abstract is assumed to be unlimited.